Binary Black Holes mergers from Population III stars

Filippo Santoliquido

Collaborators: Marica Branchesi, Jan Harms, Ulyana Dupletsa, Jacopo Tissino, Giuliano Iorio, Michela Mapelli, M. Celeste Artale *et al.*

Universidad Andrés Bello — August 6, 2024

GRAN SASSO SCIENCE INSTITUTE SCHOOL OF ADVANCED STUDIES Scuola Universitaria Superiore

GSSI team

And many others…

Contact me at filippo.santoliquido@gssi.it or visit https://filippo-santoliquido.github.io/

Gravitational Wave Astrophysics

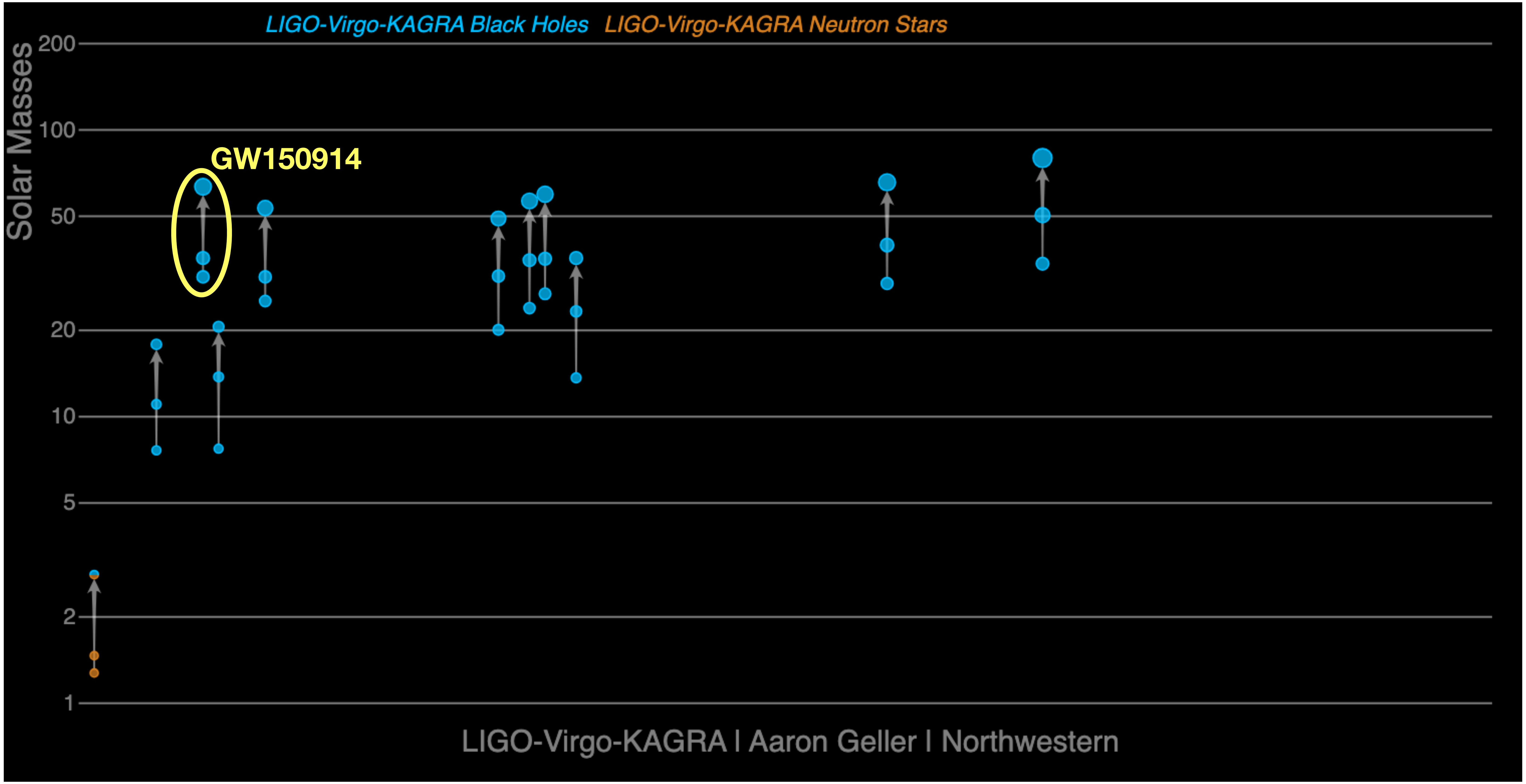

Gravitational Wave Astrophysics

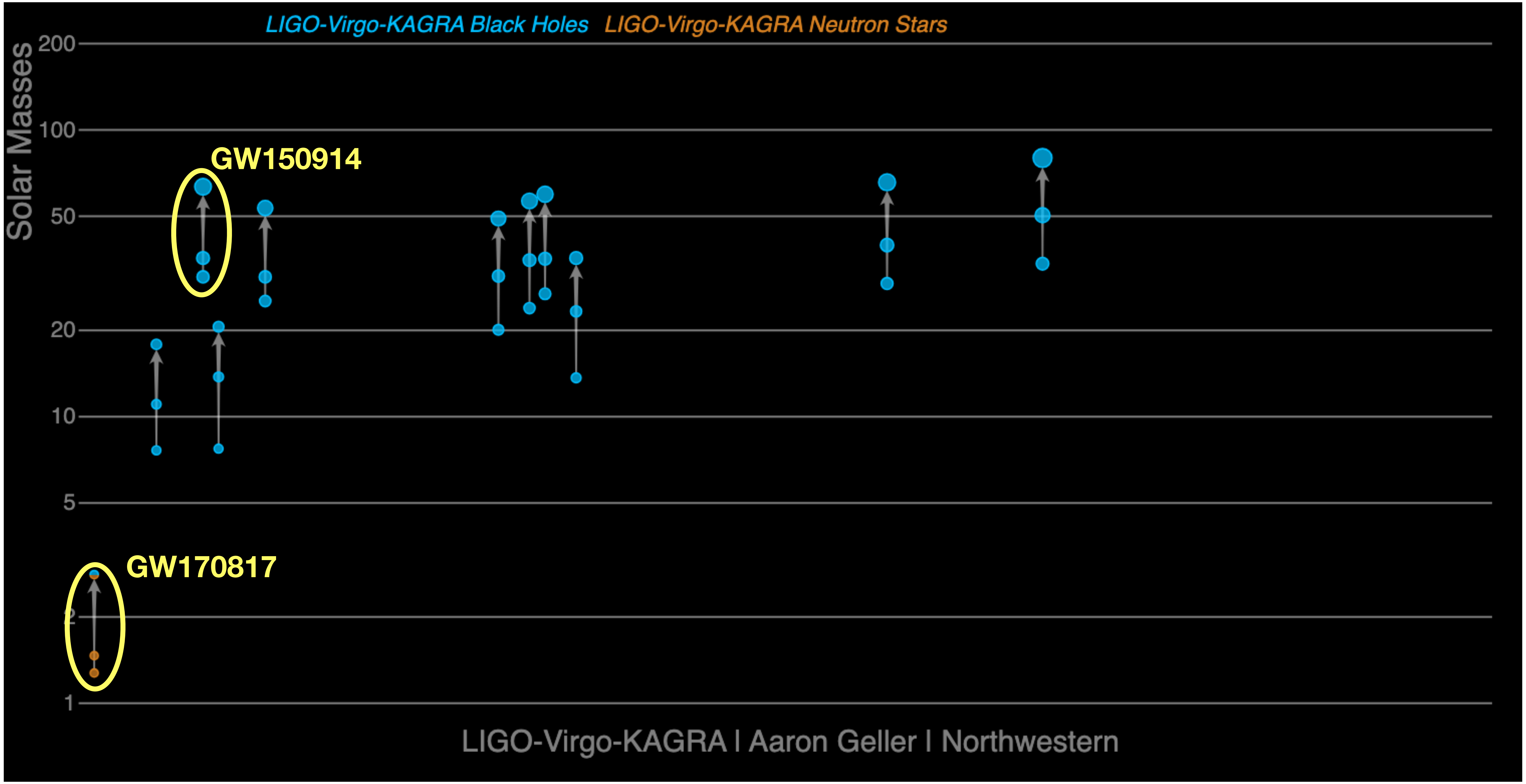

Gravitational Wave Astrophysics

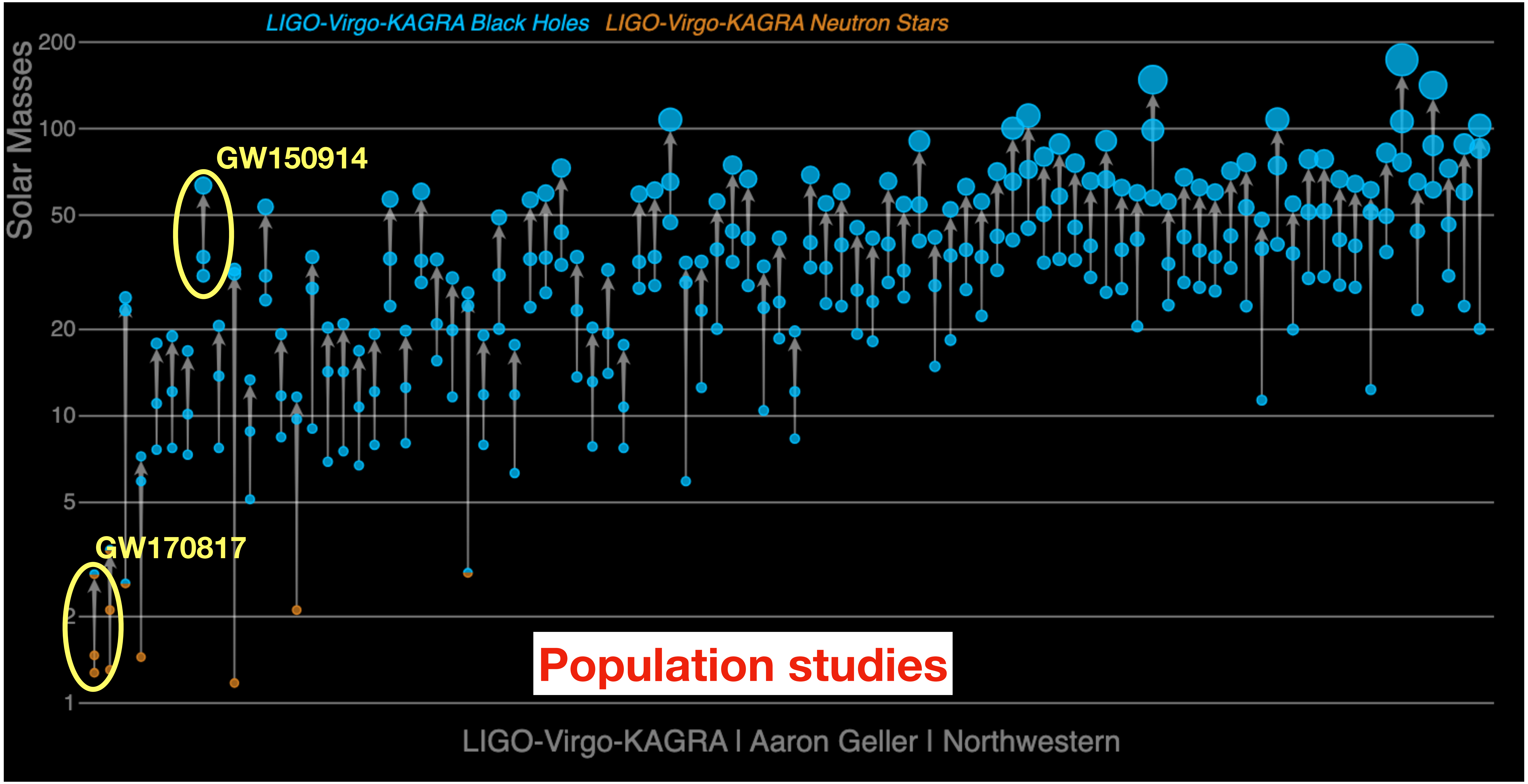

Refs: Abbott et al. 2023, Abbott et al. 2024

Filippo Santoliquido

Merger rate density

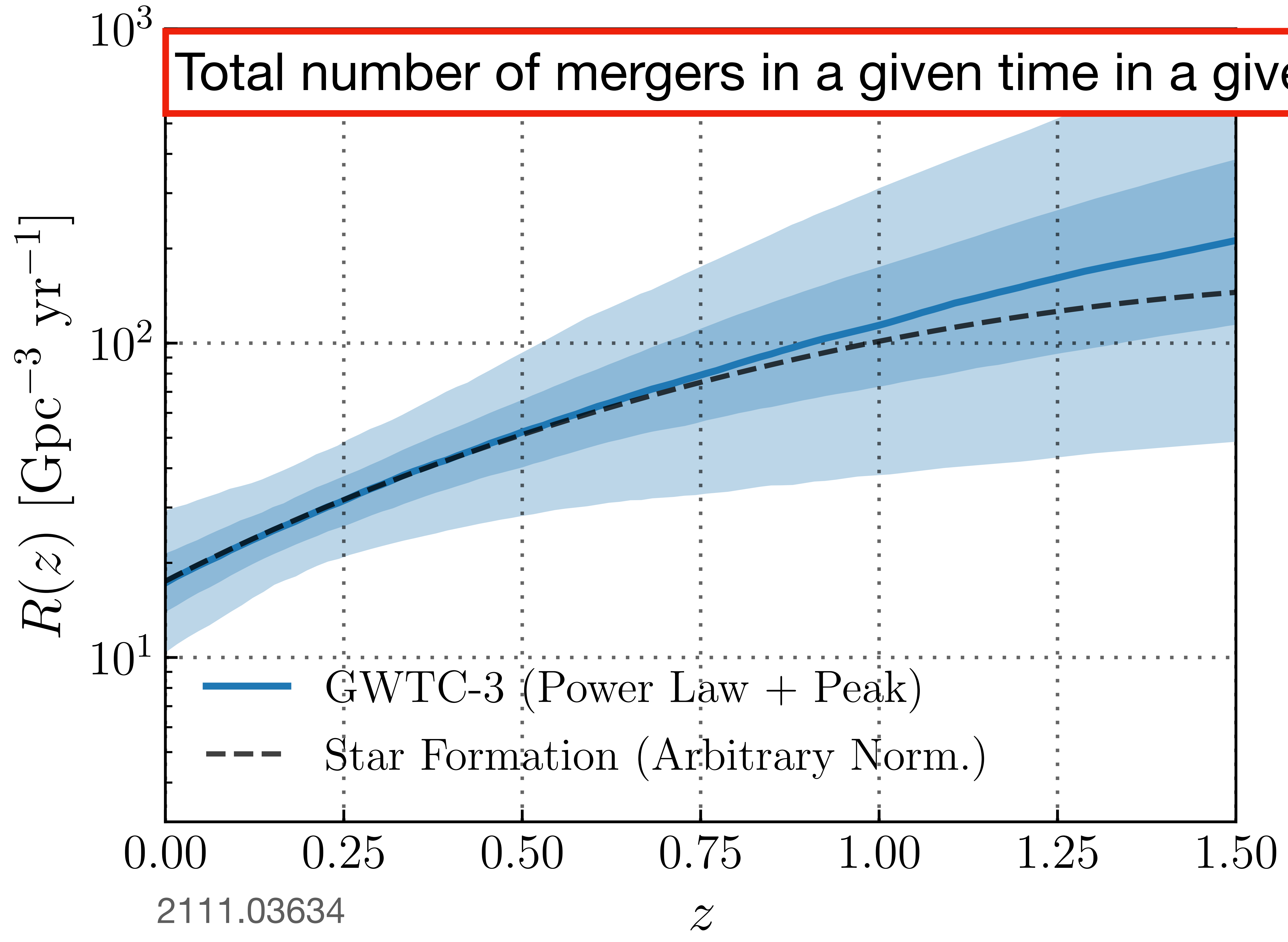

2111.03634

Total number of mergers in a given time in a given volume

- $\mathscr{R}(z) = \mathscr{R}^0(1+z)^\kappa$
- $\kappa > 0$ at 99% credibility

Merger rate density

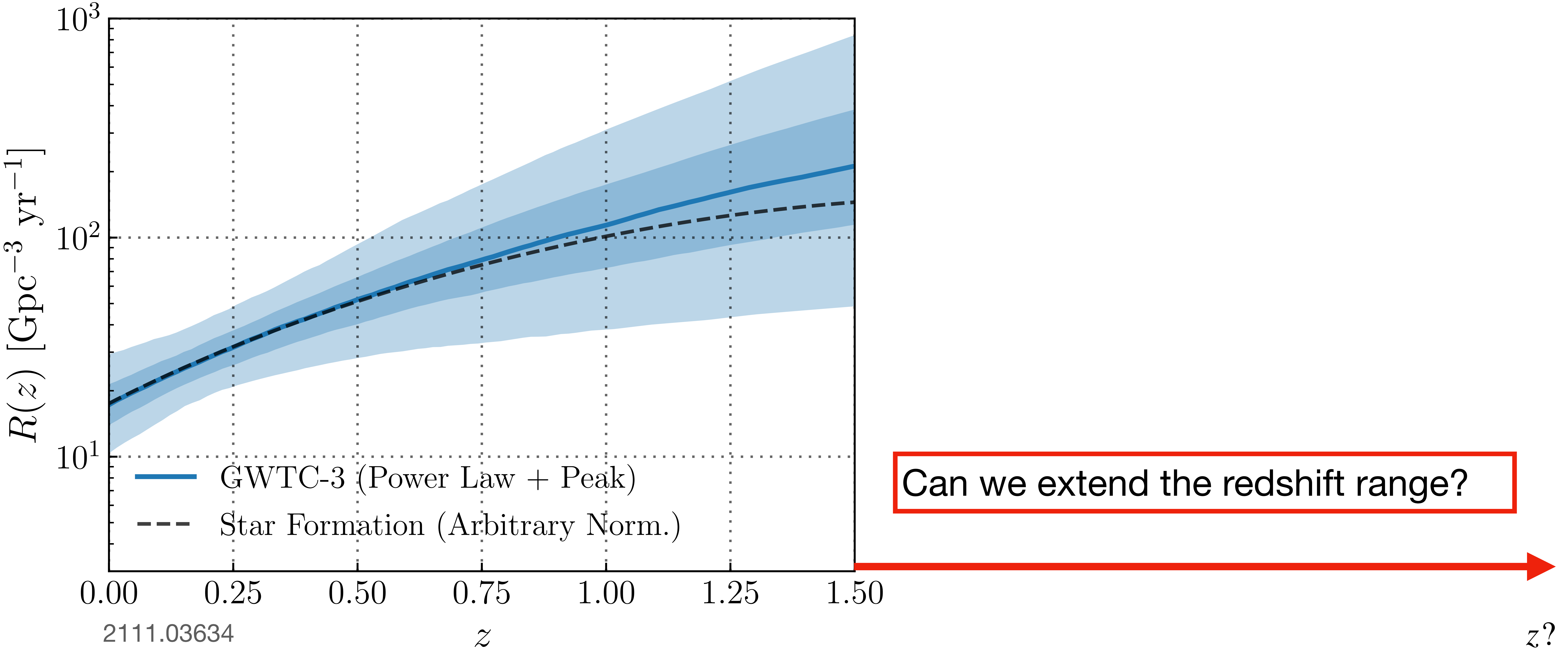

2111.03634

Can we extend the redshift range?

The Einstein Telescope

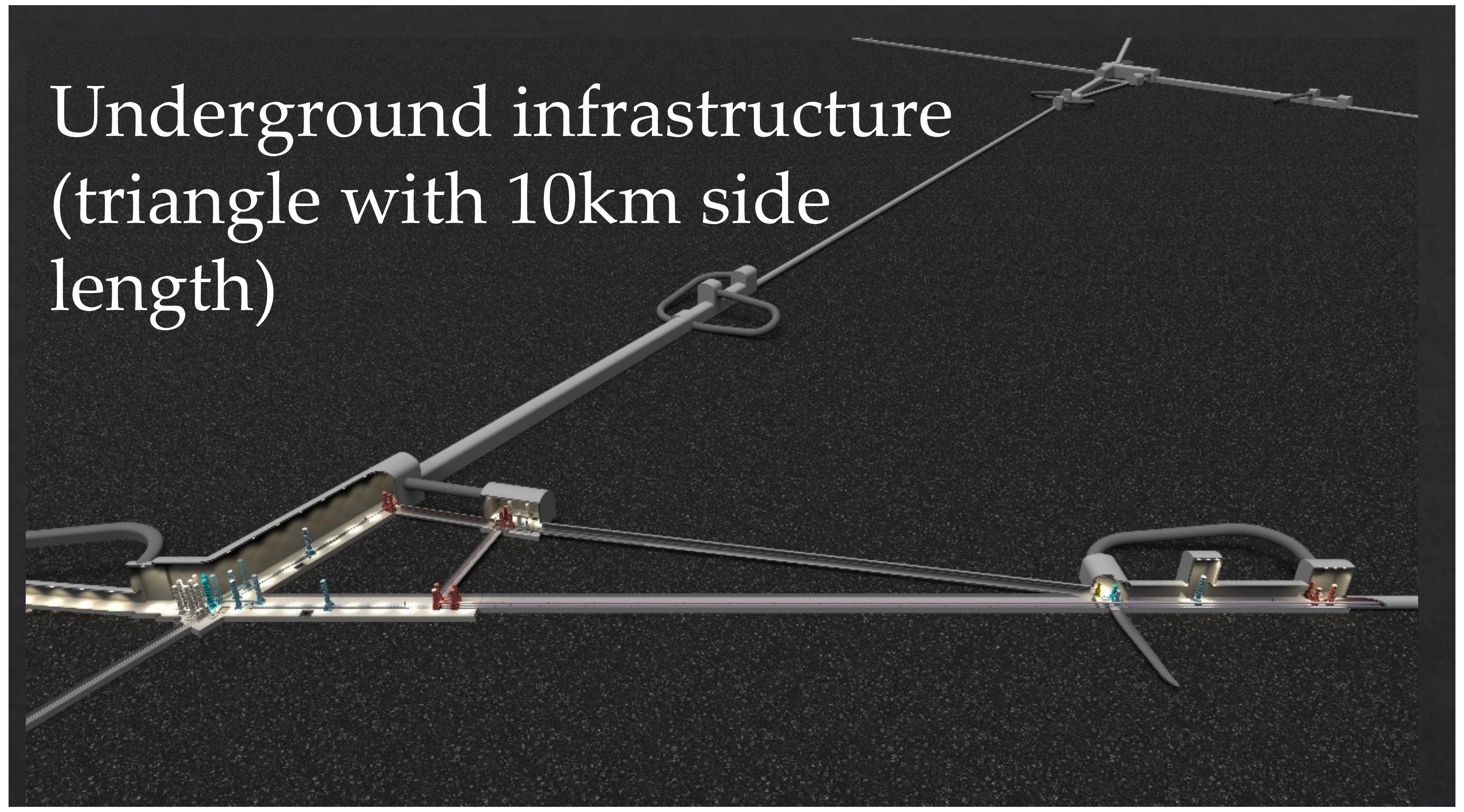

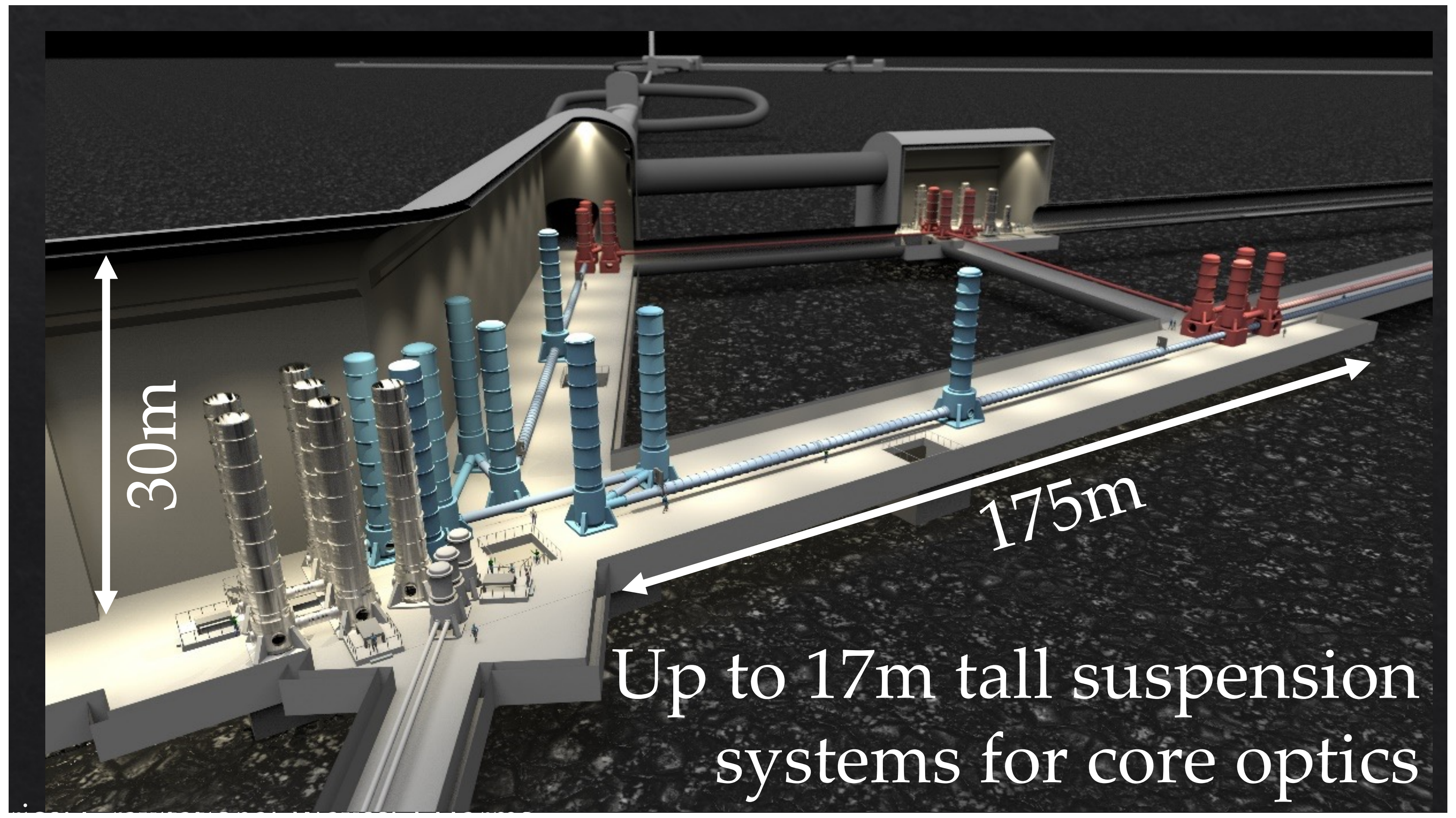

Credits: Jan Harms

Third-generation detectors

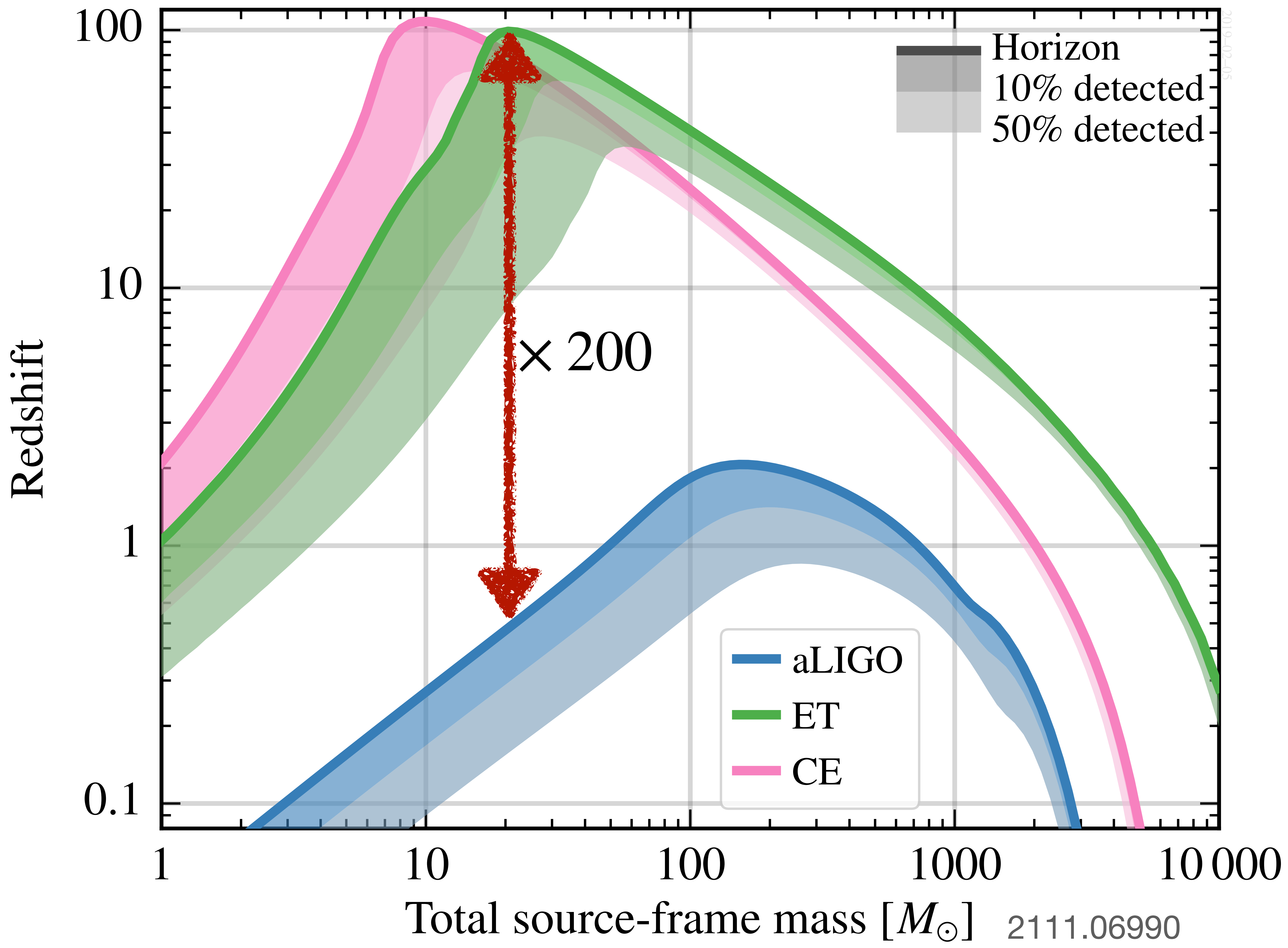

2111.06990

Population III stars

- Population III stars are believed to be the first generation of stars formed at **high redshift** $(z > 20)$

- They are massive and formed from pristine gas (i.e. **zero metallicity**)

- They are still undetected *(traces of their existence with JWST)*

- Modelled through cosmological simulations

Ref. ***Klessen & Glover 2023***, ***Bromm & Larson 2004***, ***Zackrisson et al. 2023***, ***Maiolino et al. 2024***

Our goals

- Large parameter space exploration of Pop. III BBHs
- Merger rate density
- Evolution of mass spectrum with redshift
- Expected detection rates with the Einstein Telescope

Isolated formation channel

- Two massive stars form in the **same binary system** and evolve together

- *Let's see an example*

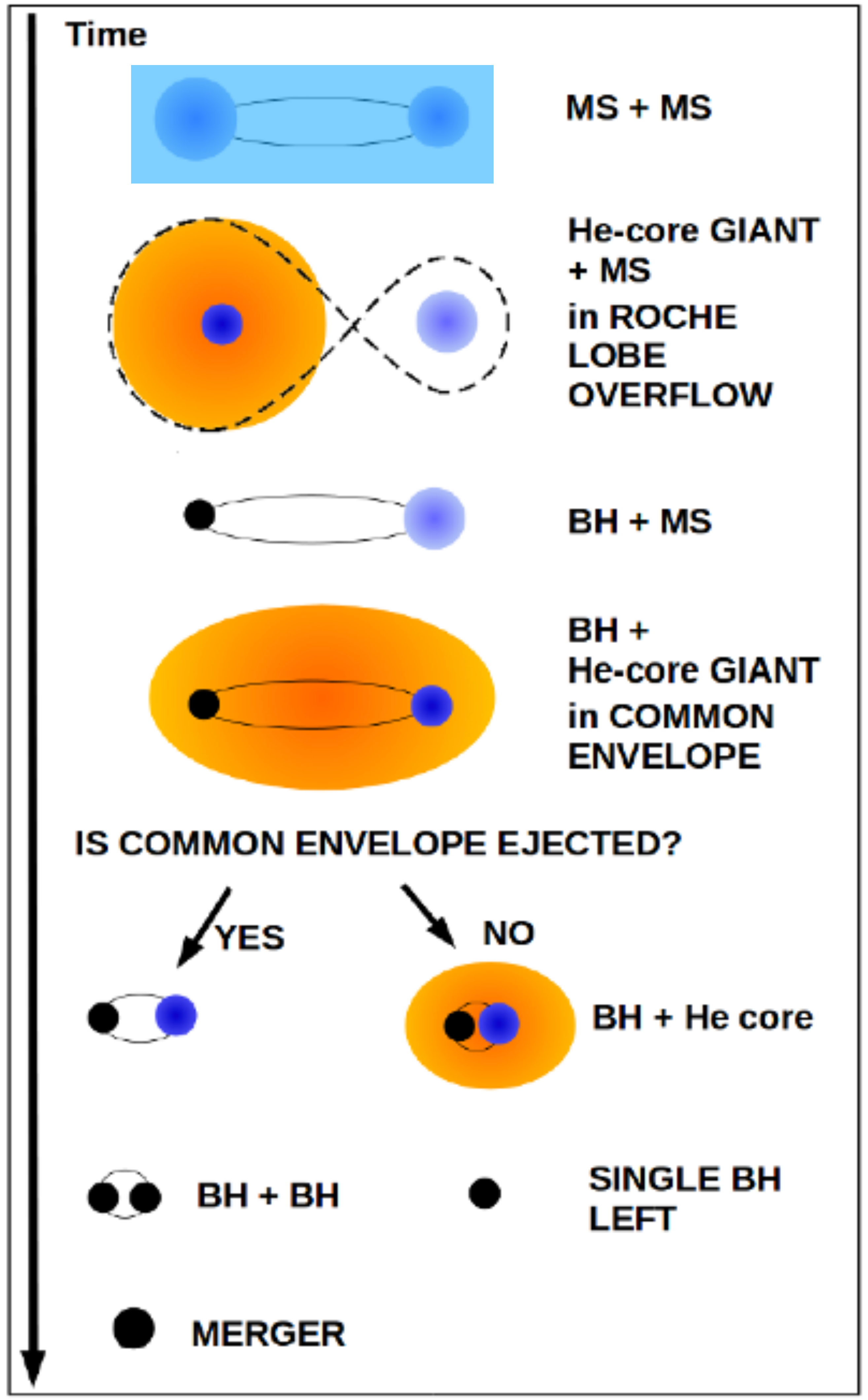

Isolated formation channel

- Following radius expansion, one star can fill its Roche lobe

- Mass can be transferred to the other in a **stable mass transfer** (Roth lobe overflow)

- The orbit of the binary system shrinks due to angular momentum loss

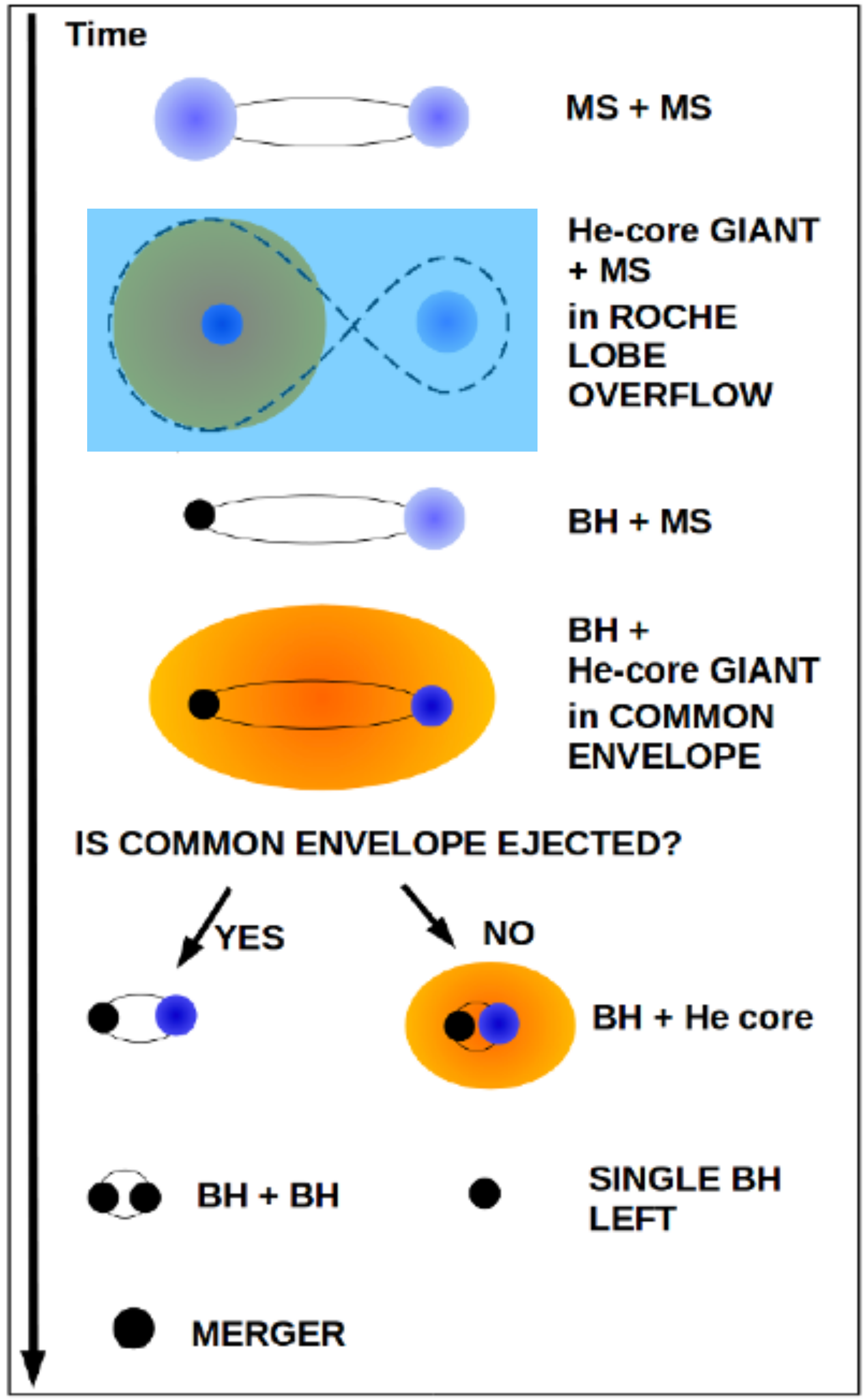

Isolated formation channel

- If $M_{\rm ZAMS} \gtrsim 20\ \rm M_{\odot}$, the first black is formed after core **collapse supernova**

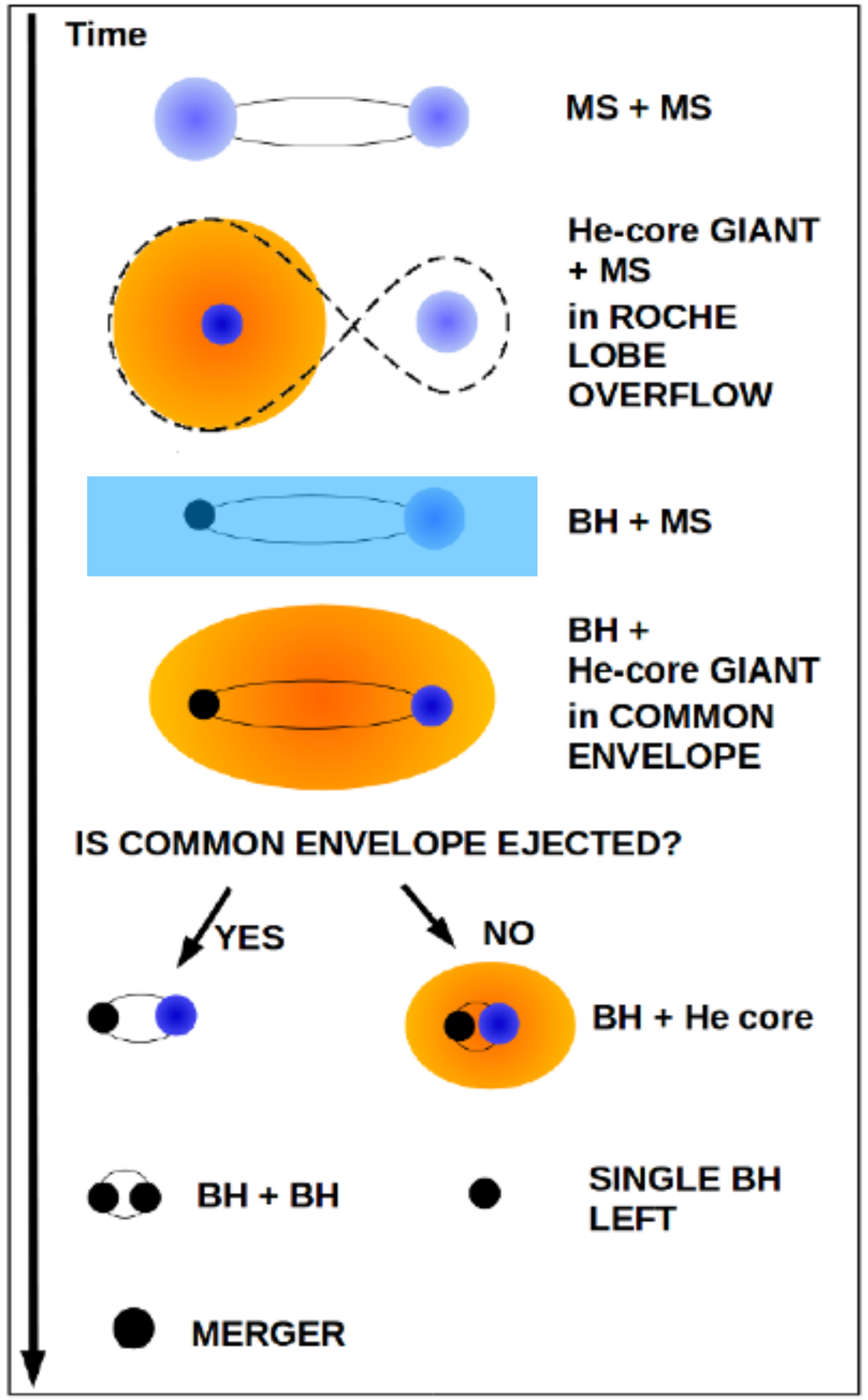

Isolated formation channel

- The other star starts transferring mass through unstable mass transfer
- Beginning of the **common envelope** phase
- A drag force is exerted between the black hole and the stellar core.
- Orbital energy is transferred to the common envelope that is eventually ejected, shrinking the binary system

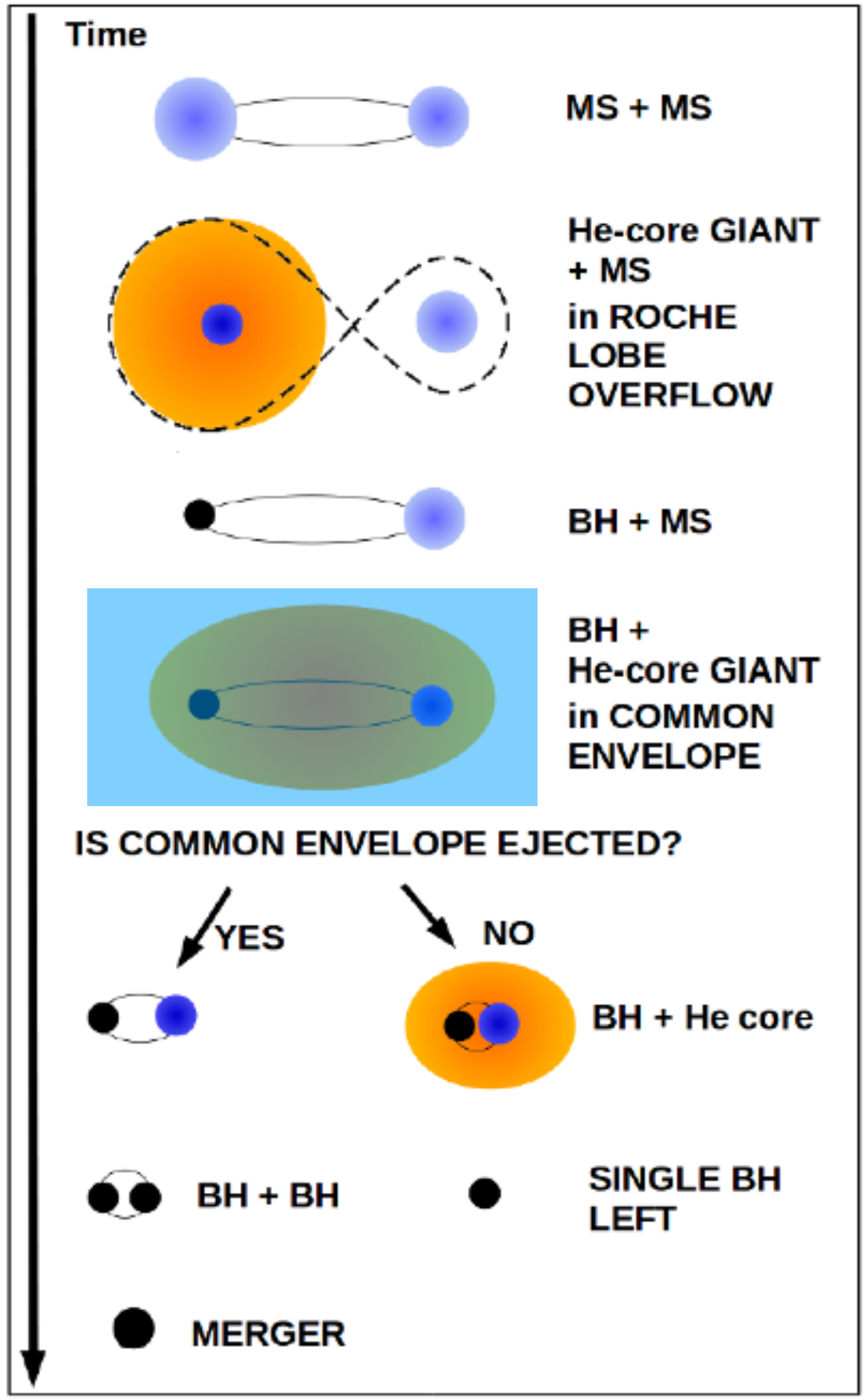

Ref. *Mapelli 2018*, *Spera et al. 2022*, *Costa et al. 2023*

Credits: Michela Mapelli

Isolated formation channel

- If $M_{\mathrm{ZAMS}} \gtrsim 20\ \mathrm{M}_{\odot}$, the second black hole forms
- The binary system starts to loose energy through **gravitational wave radiation emission**
- The **two black holes** might eventually **merge** within an Hubble time

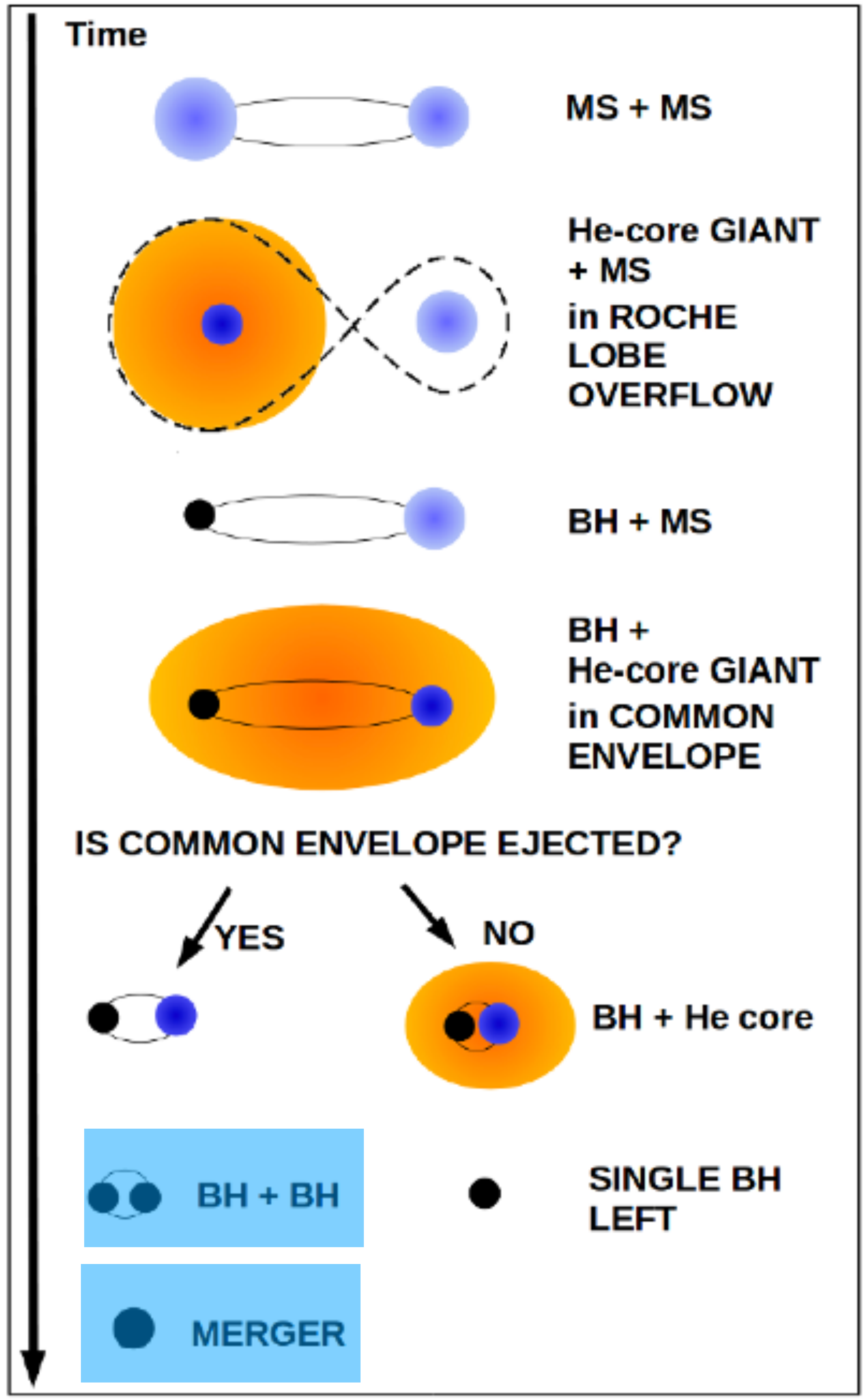

Ref. *Mapelli 2018*, *Spera et al. 2022*, *Costa et al. 2023*

Credits: Michela Mapelli

Population synthesis

- SEVN: population-synthesis code with **stellar tracks**
- *Costa et al. 2023* generated a new set of Pop. III stellar tracks
- We evolve a large set of Pop III. binary stars

Population synthesis

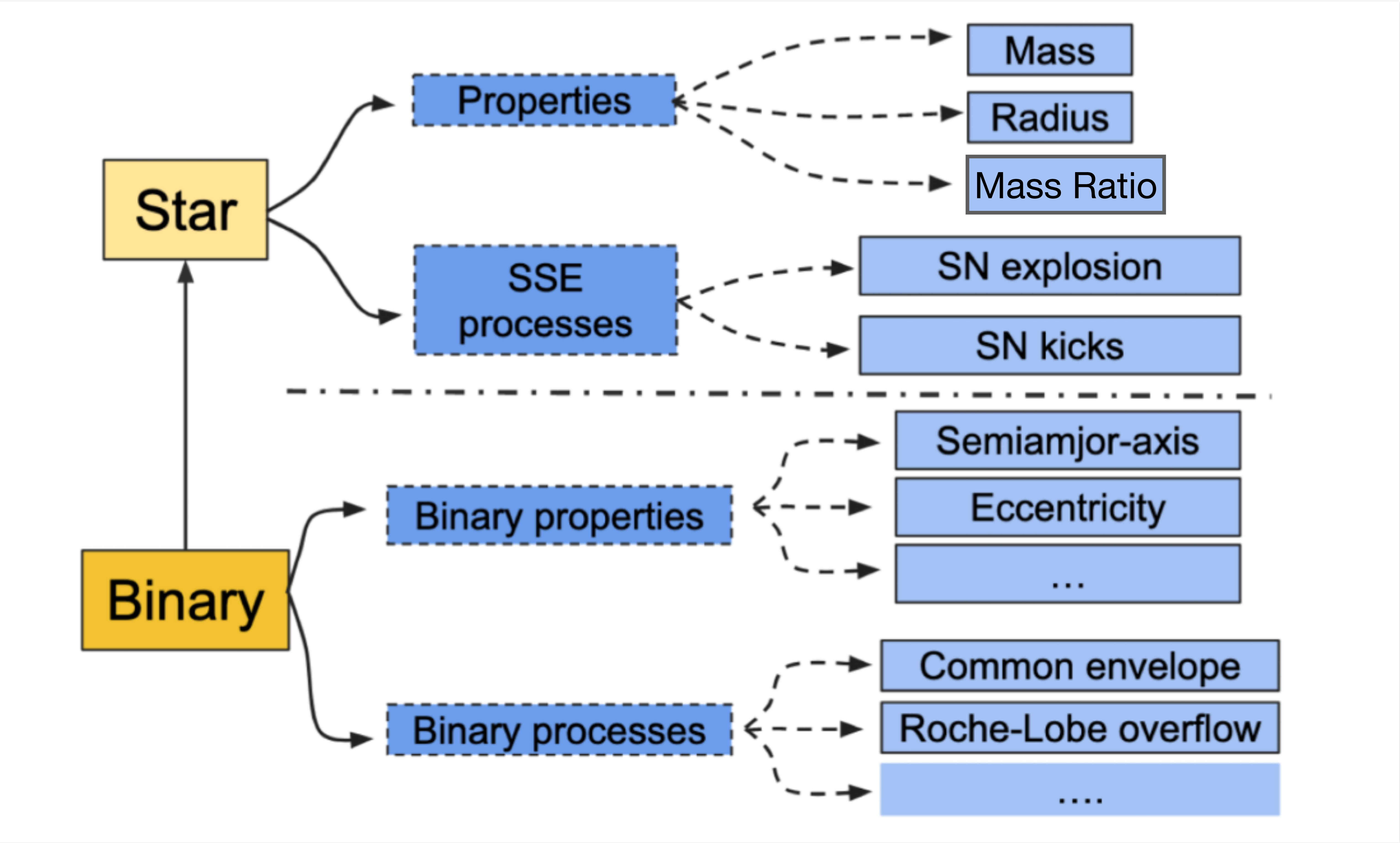

Credits: Iorio et al. 2023

Population synthesis

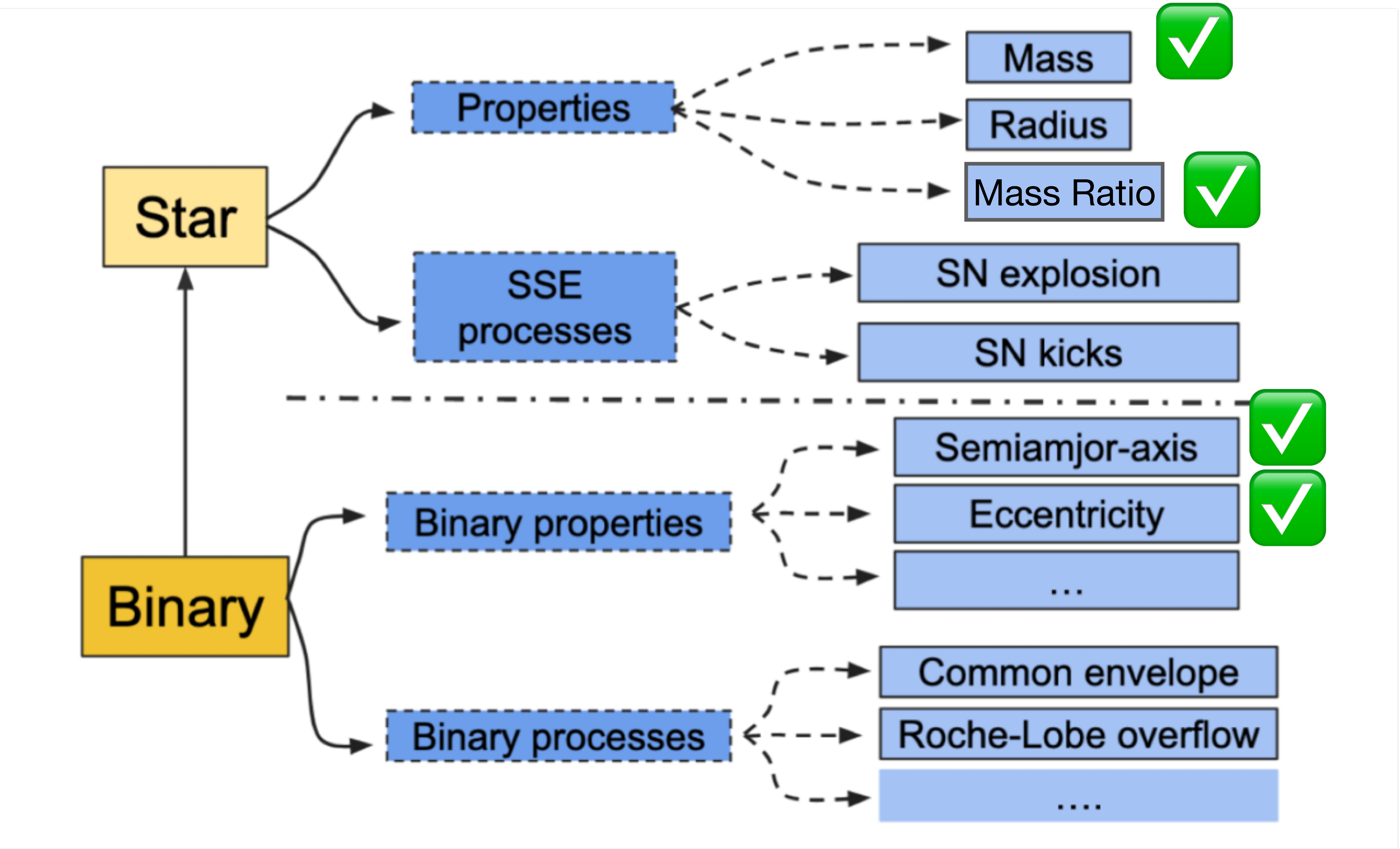

Credits: Iorio et al. 2023

Exploring initial conditions

Initial conditions

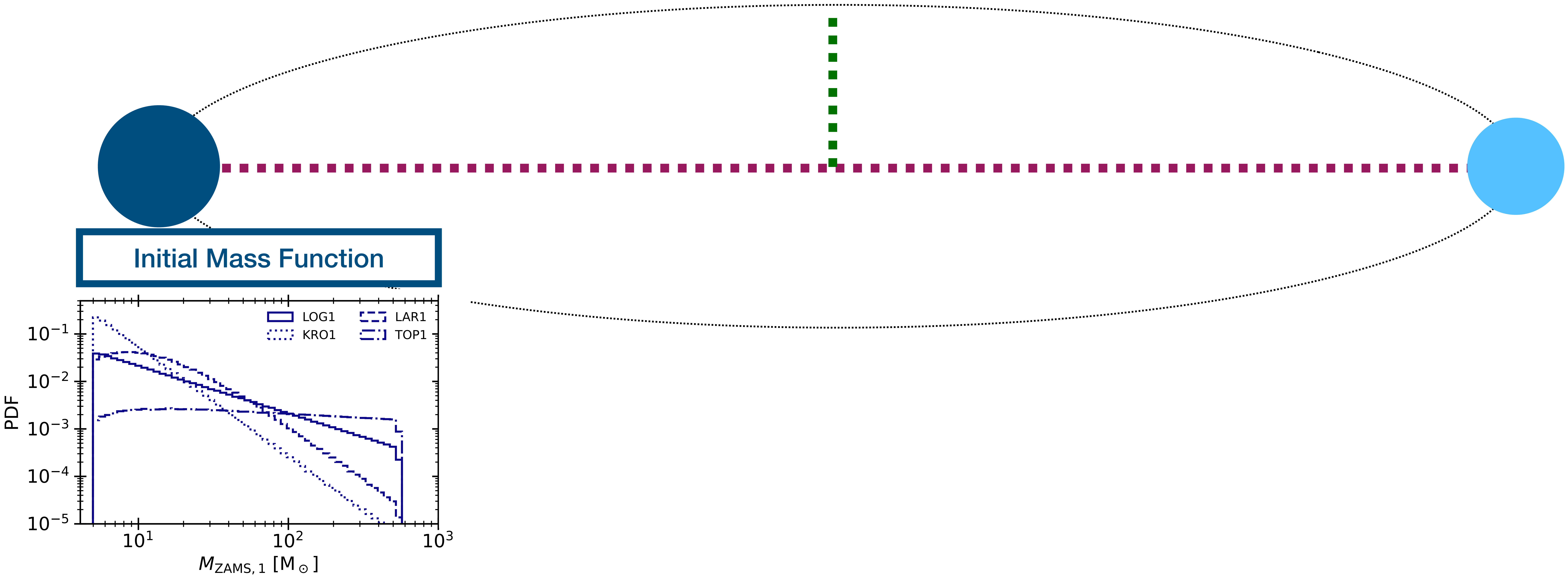

Initial conditions

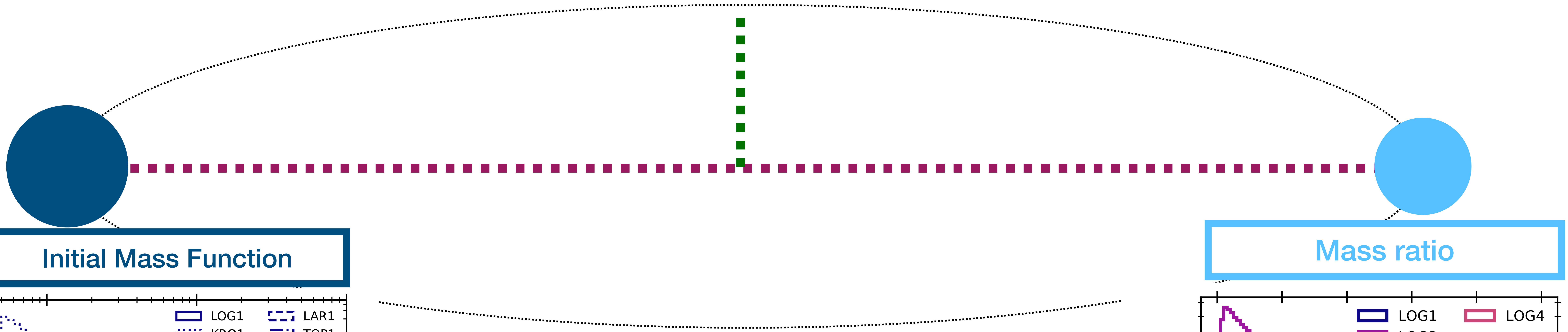

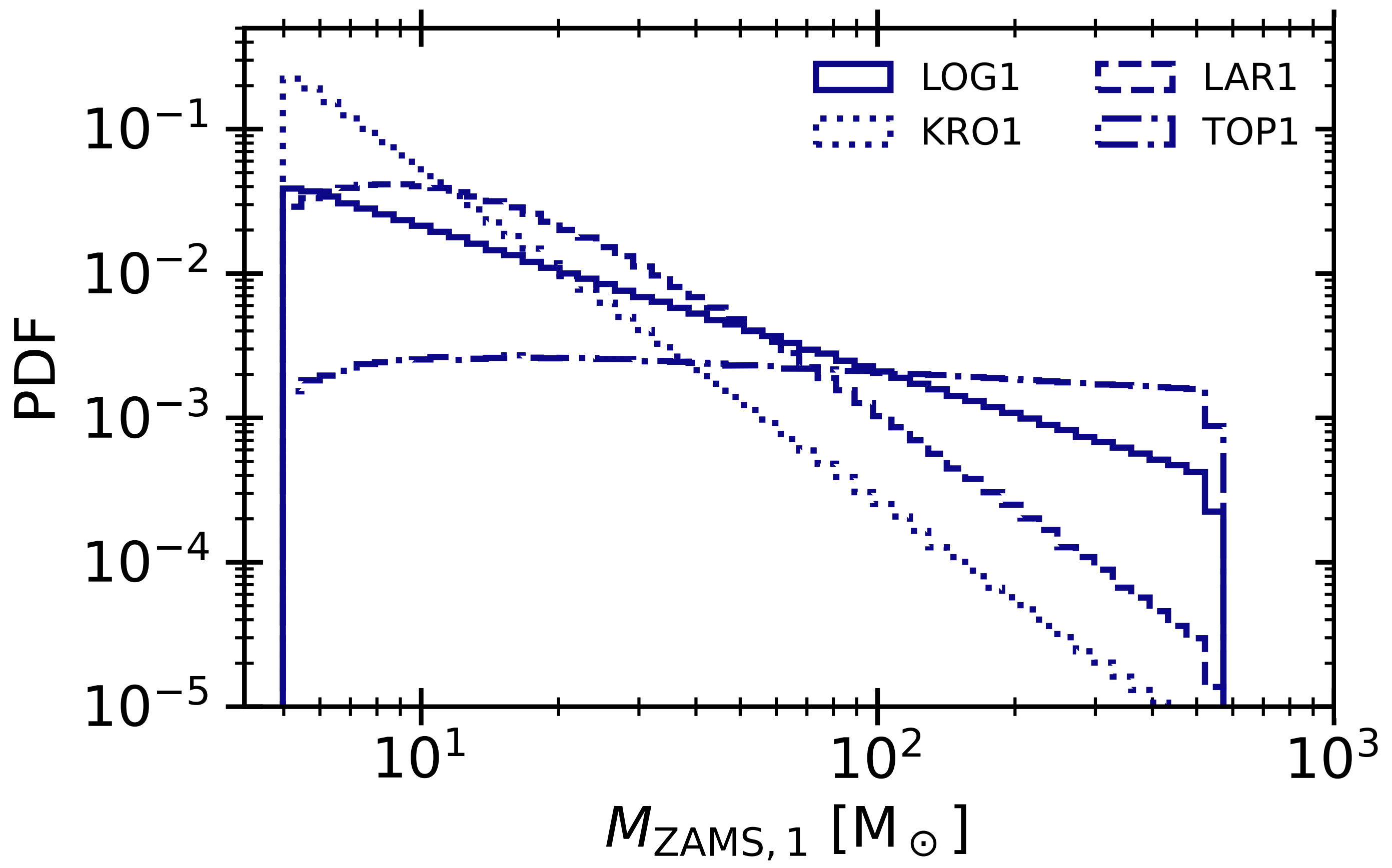

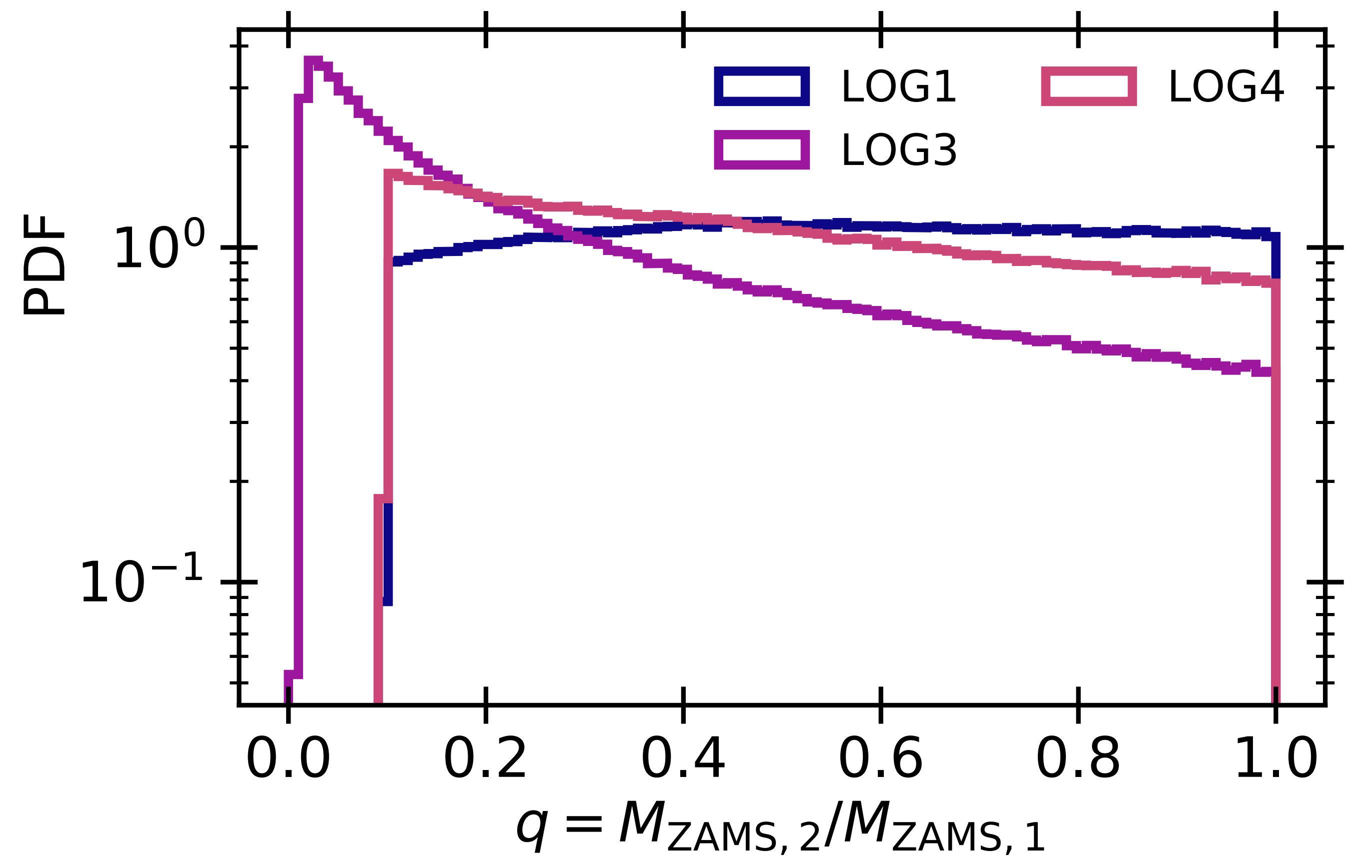

Initial conditions

COSMORATE

$$\mathcal{R}(z) = \int_{z_{\max}}^{z} \left[\int_{Z_{\min}}^{Z_{\max}} \mathrm{SFRD}(z', Z)\, \mathcal{F}(z', z, Z)\, \mathrm{d}Z \right] \frac{\mathrm{d}t(z')}{\mathrm{d}z'} \mathrm{d}z'$$

Output from SEVN

Catalogs of merging BBHs:
primary mass, secondary mass,
delay time
$z' \rightarrow z$

COSMORATE

$$\mathcal{R}(z) = \int_{z_{\max}}^{z} \left[\int_{Z_{\min}}^{Z_{\max}} \mathrm{SFRD}(z', Z) \mathcal{F}(z', z, Z) \mathrm{d}Z \right] \frac{\mathrm{d}t(z')}{\mathrm{d}z'} \mathrm{d}z'$$

$$\mathrm{SFRD}(z, Z) = \psi(z)\, p(Z|z)$$

Evaluated from SEVN catalogs

$$Z = 10^{-11}$$

COSMORATE

$$\mathcal{R}(z) = \int_{z_{\max}}^{z} \left[\int_{Z_{\min}}^{Z_{\max}} \mathrm{SFRD}(z', Z)\, \mathcal{F}(z', z, Z)\, \mathrm{d}Z \right] \frac{\mathrm{d}t(z')}{\mathrm{d}z'} \mathrm{d}z'$$

$$\mathrm{SFRD}(z, Z) = \psi(z)\, p(Z|z)$$

Evaluated from SEVN catalogs

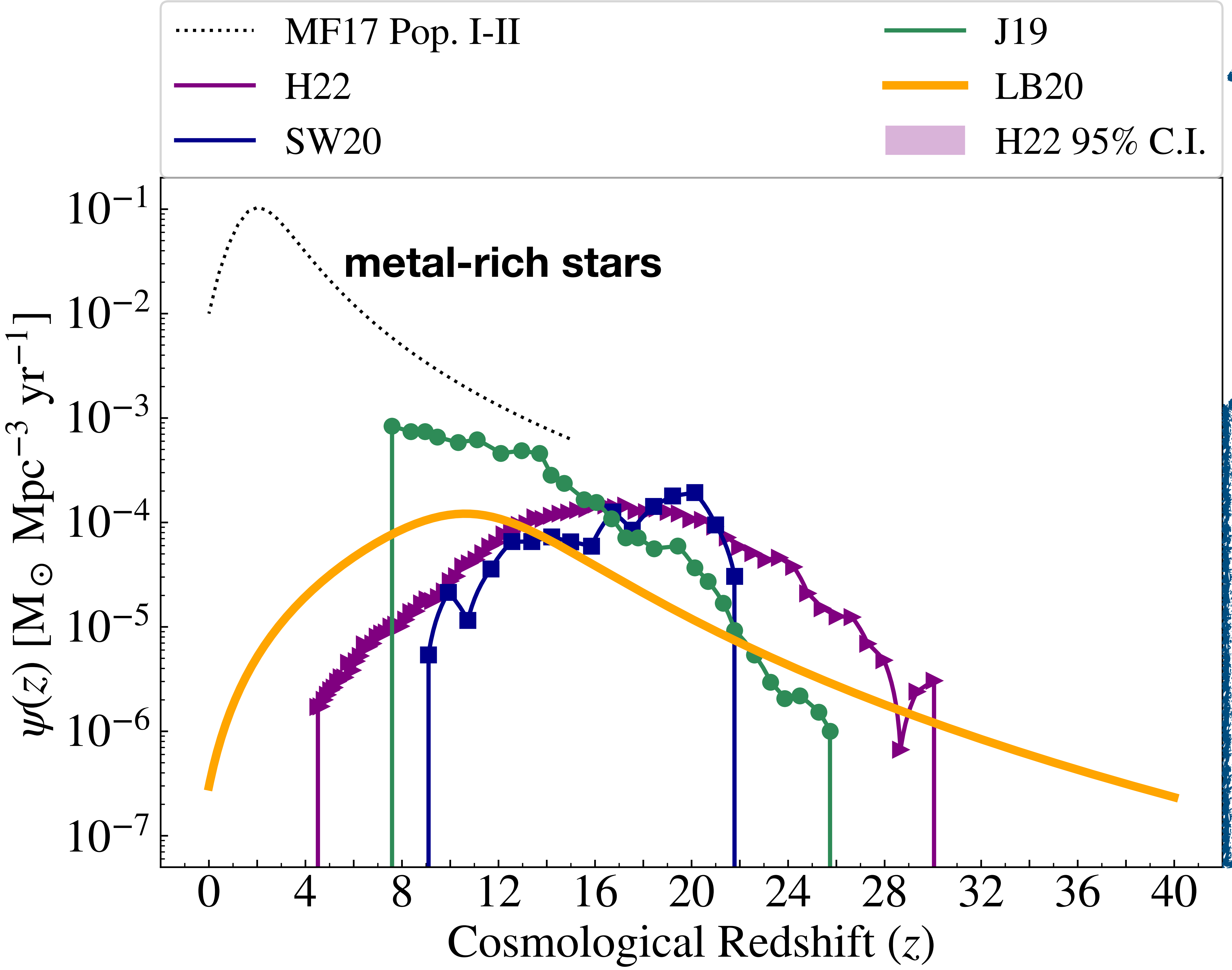

4 different Pop. III SFRDs:

H22 - *Hartwig et al. 2022*

J19 - *Jaacks et al. 2019*

LB20 - *Liu & Bromm 2020*

SW20 - *Skinner & Wise 2020*

different assumptions on baryonic physics + cosmic variance

Ref. *Santoliquido et al. 2020*, *Santoliquido et al. 2023*

Merger rate density

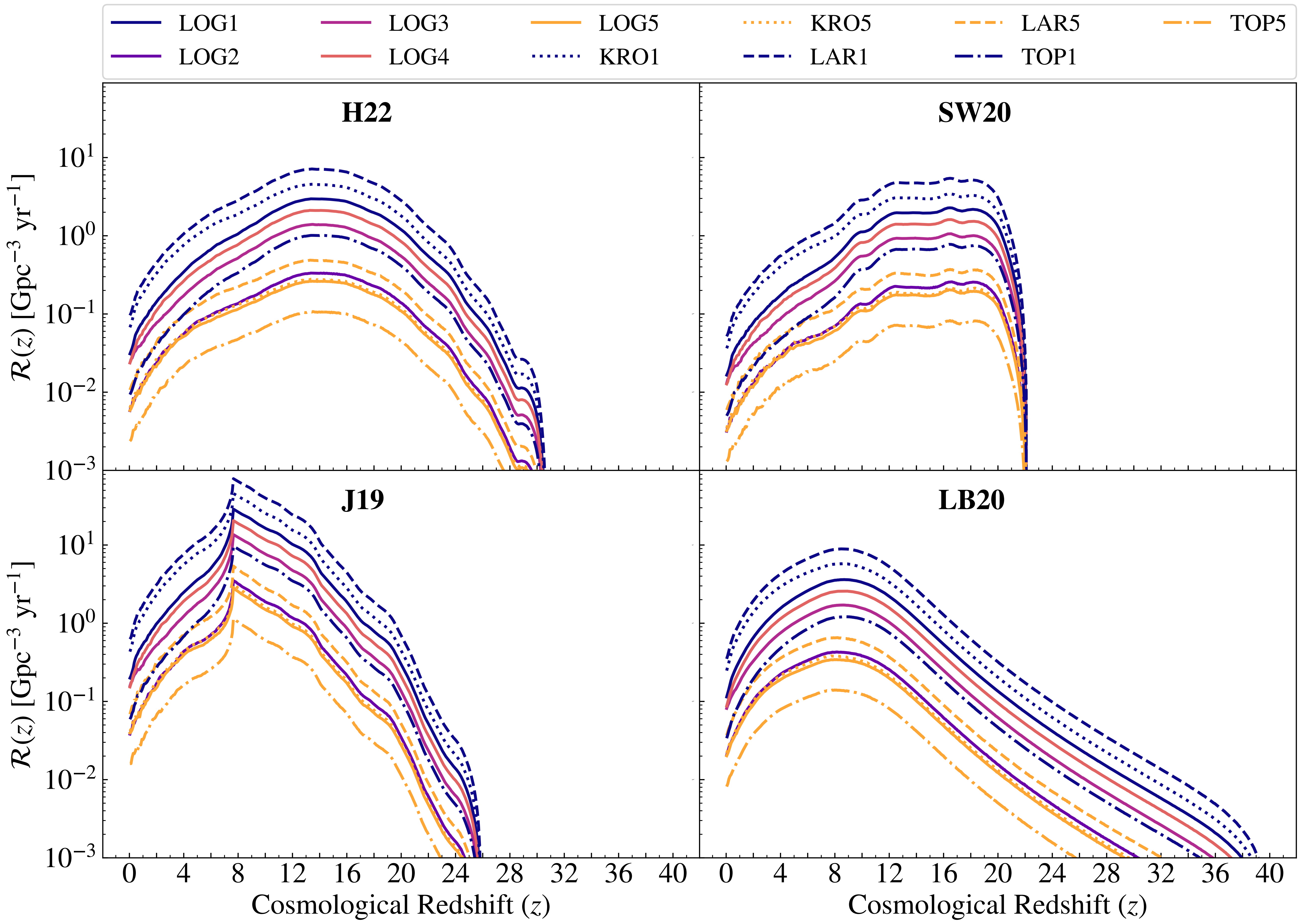

Merger rate density

initial conditions

impact ~2 orders of magnitude

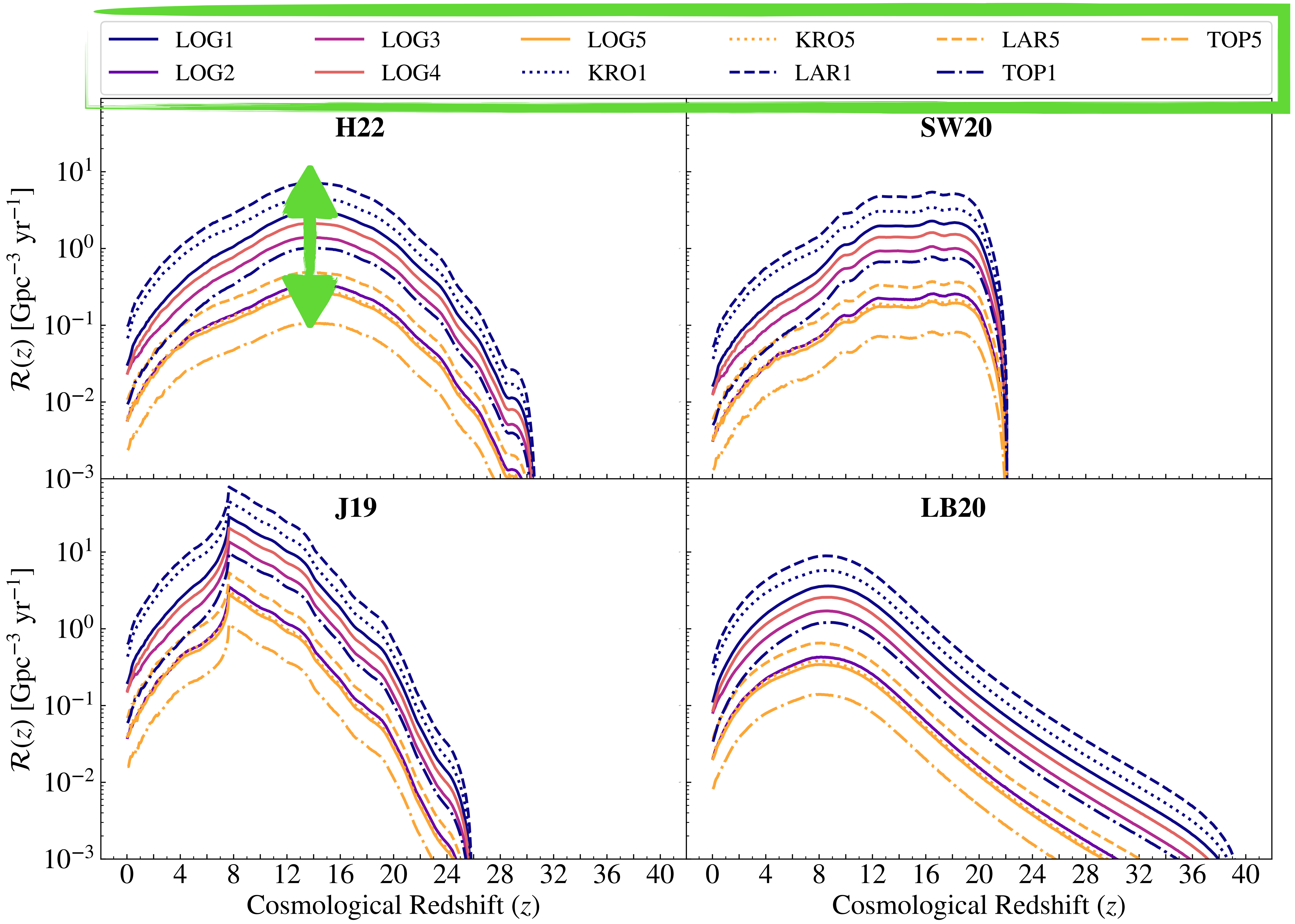

Merger rate density

star formation history impacts shape and normalisation

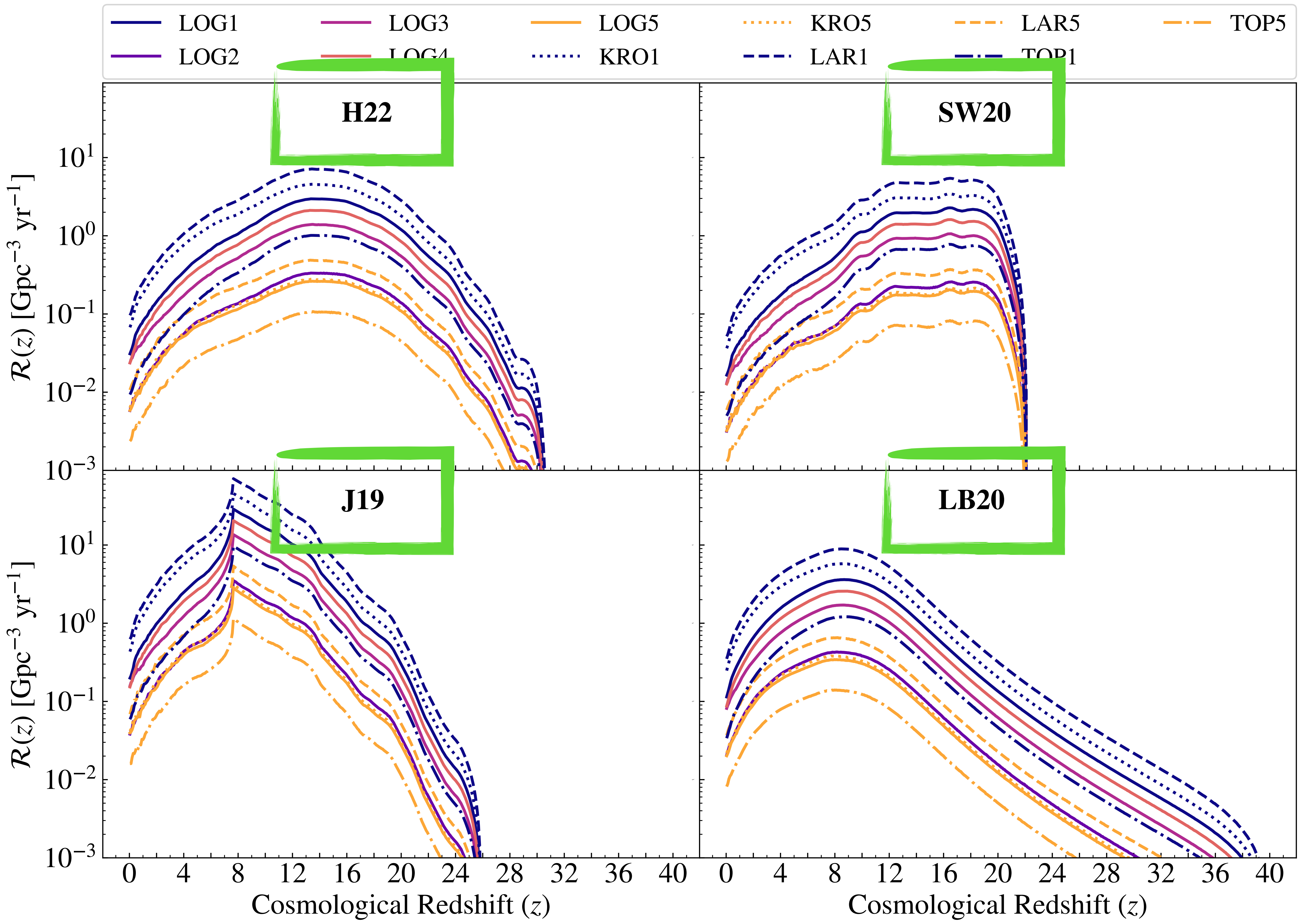

Primary mass

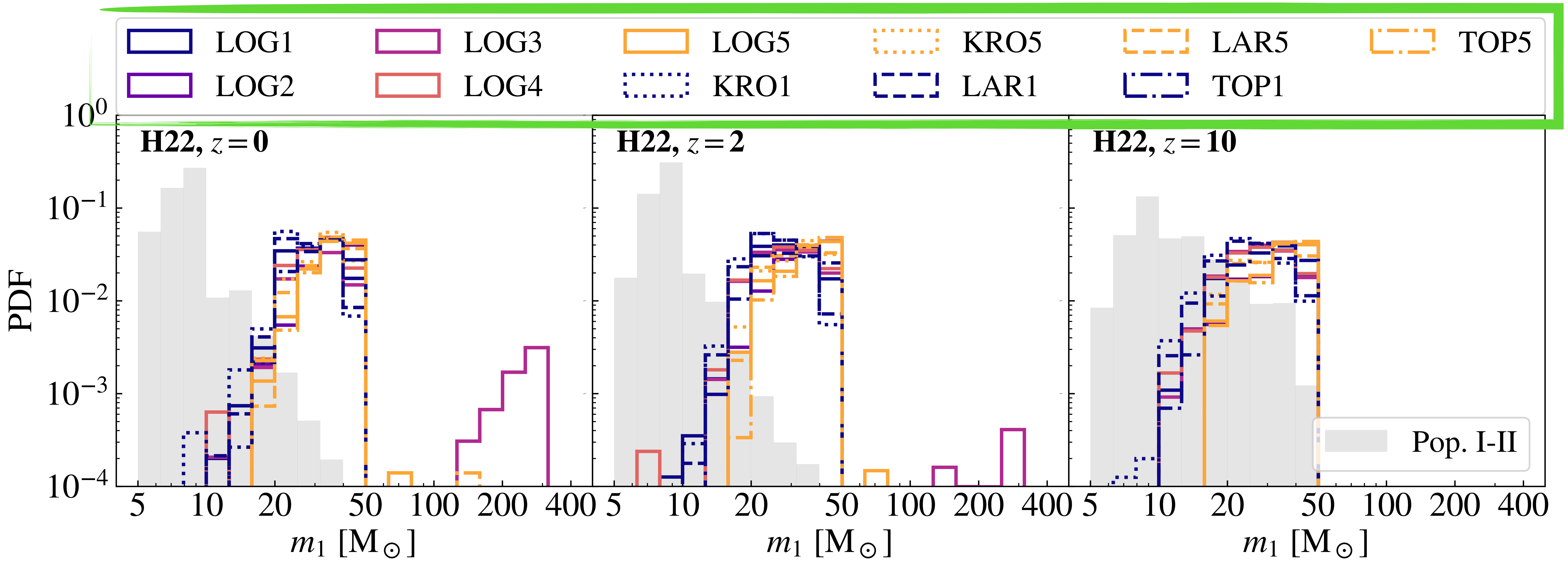

Primary mass

At $z = 0$, **Pop. I-II** BBHs show a **main peak at 8 – 10** $\mathrm{M}_\odot$

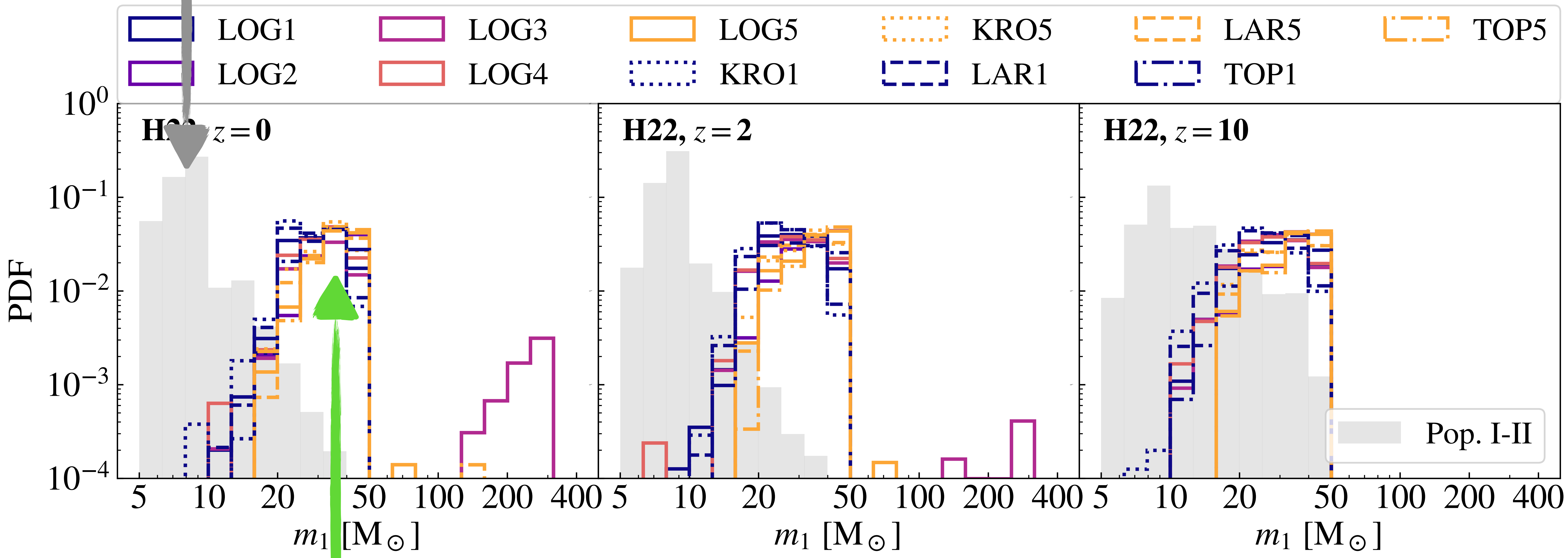

Pop. III BBHs show a **main peak at 30 – 35** $\mathrm{M}_\odot$

Primary mass

At $z = 0$, **Pop. I-II** BBHs show a **main peak at 8 – 10** $M_\odot$

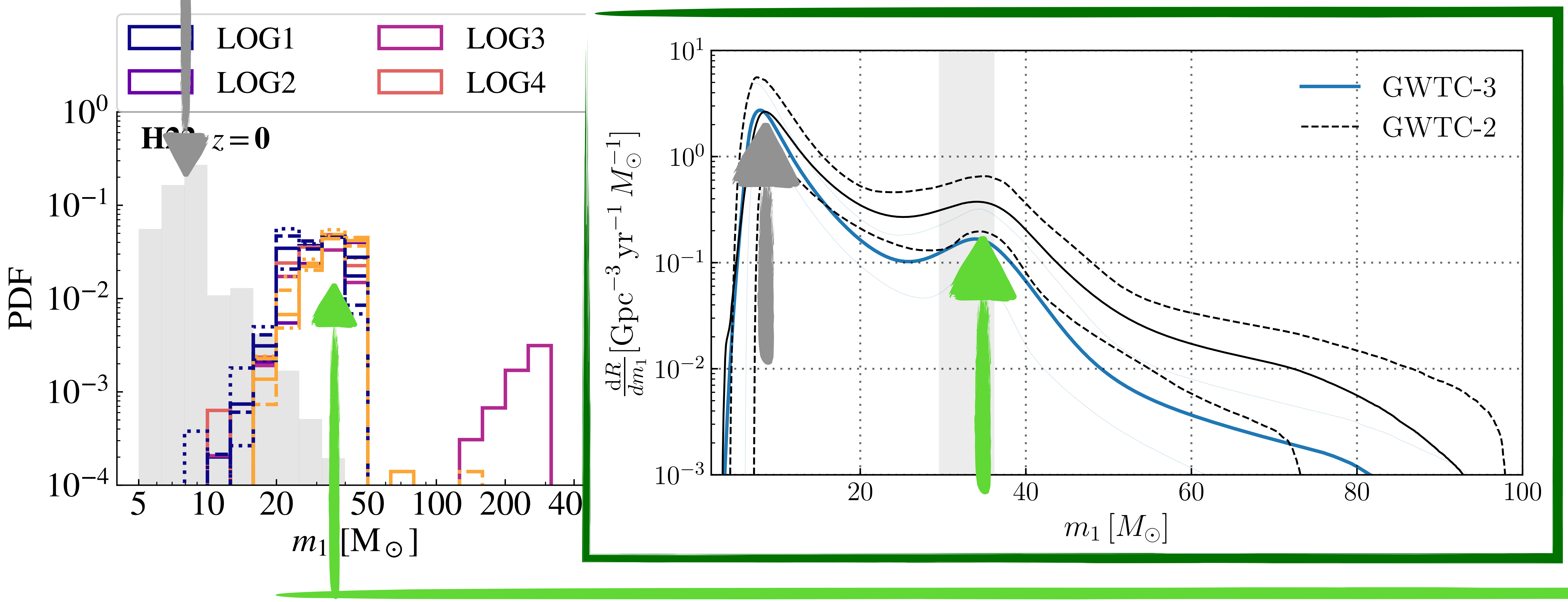

Pop. III BBHs show a **main peak at 30 – 35** $M_\odot$

Primary mass

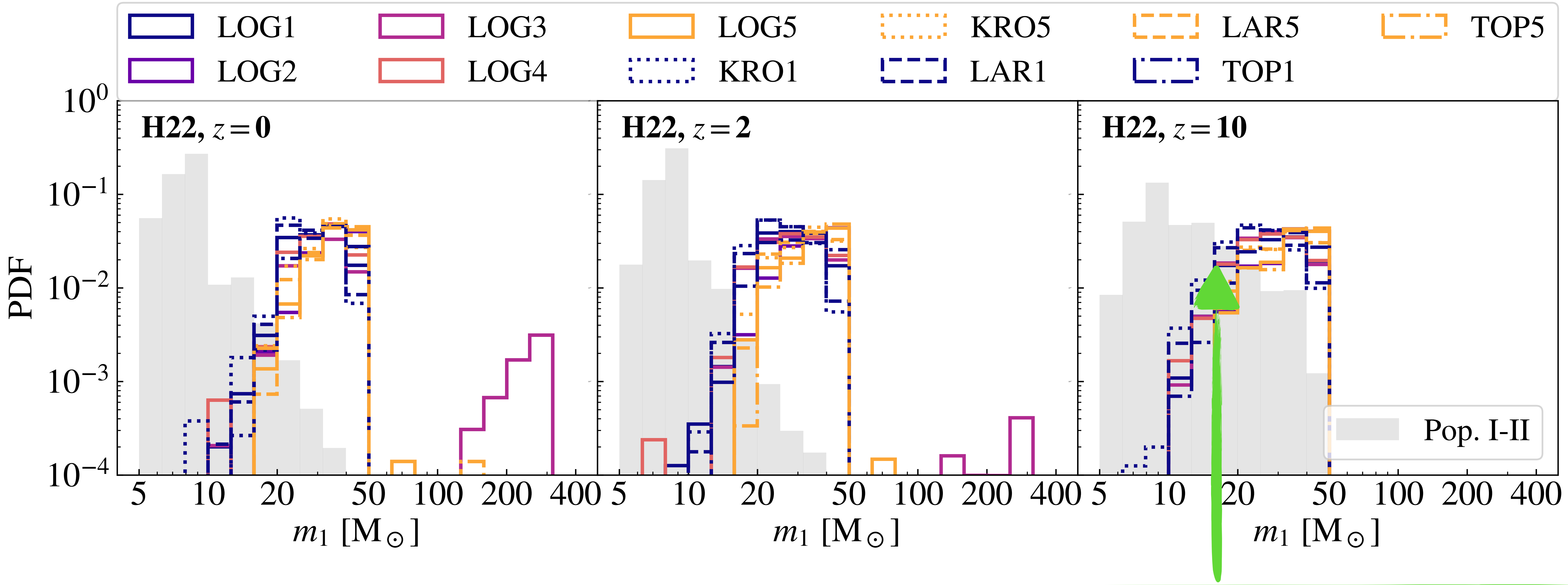

At high redshift, overlap increases

Detection rate

- Einstein Telescope will detect 10 – 10^4 Pop. III BBH mergers per year
- We expect between 23% and 73% of detections to occur at redshift $z > 8$

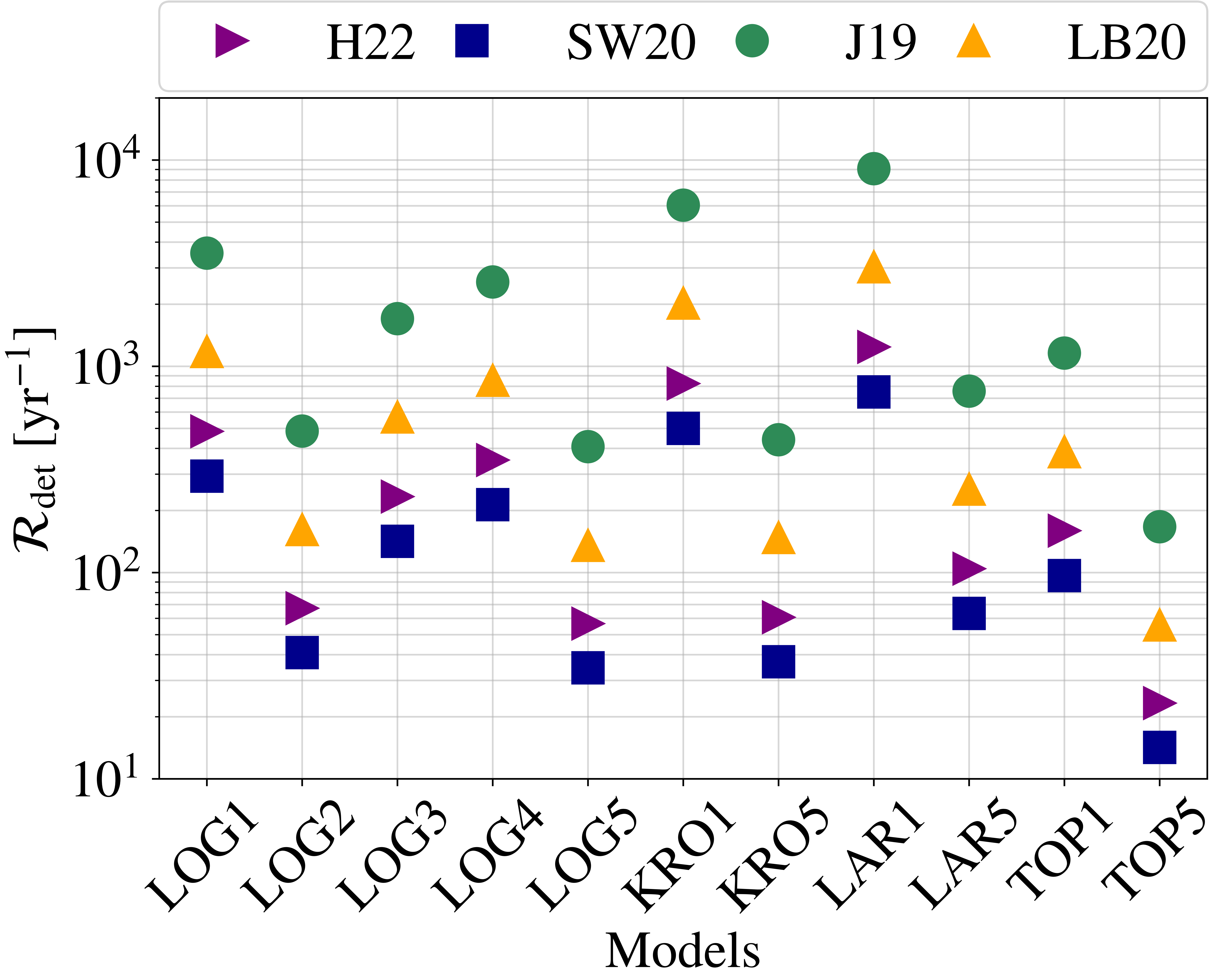

Can we distinguish Pop. III BBHs?

- Einstein Telescope will detect BBH mergers up to $z \sim 100$
- high-redshift sources with low-SNR and poor estimate of d_{L}
- inferring the origin of individual GW detections will not be granted

Ref. ***Maggiore et al. 2020***, ***Ng et al. 2021***, ***2022***, ***Branchesi et al. 2023***, ***Mancarella et al. 2023***

Goal: classification

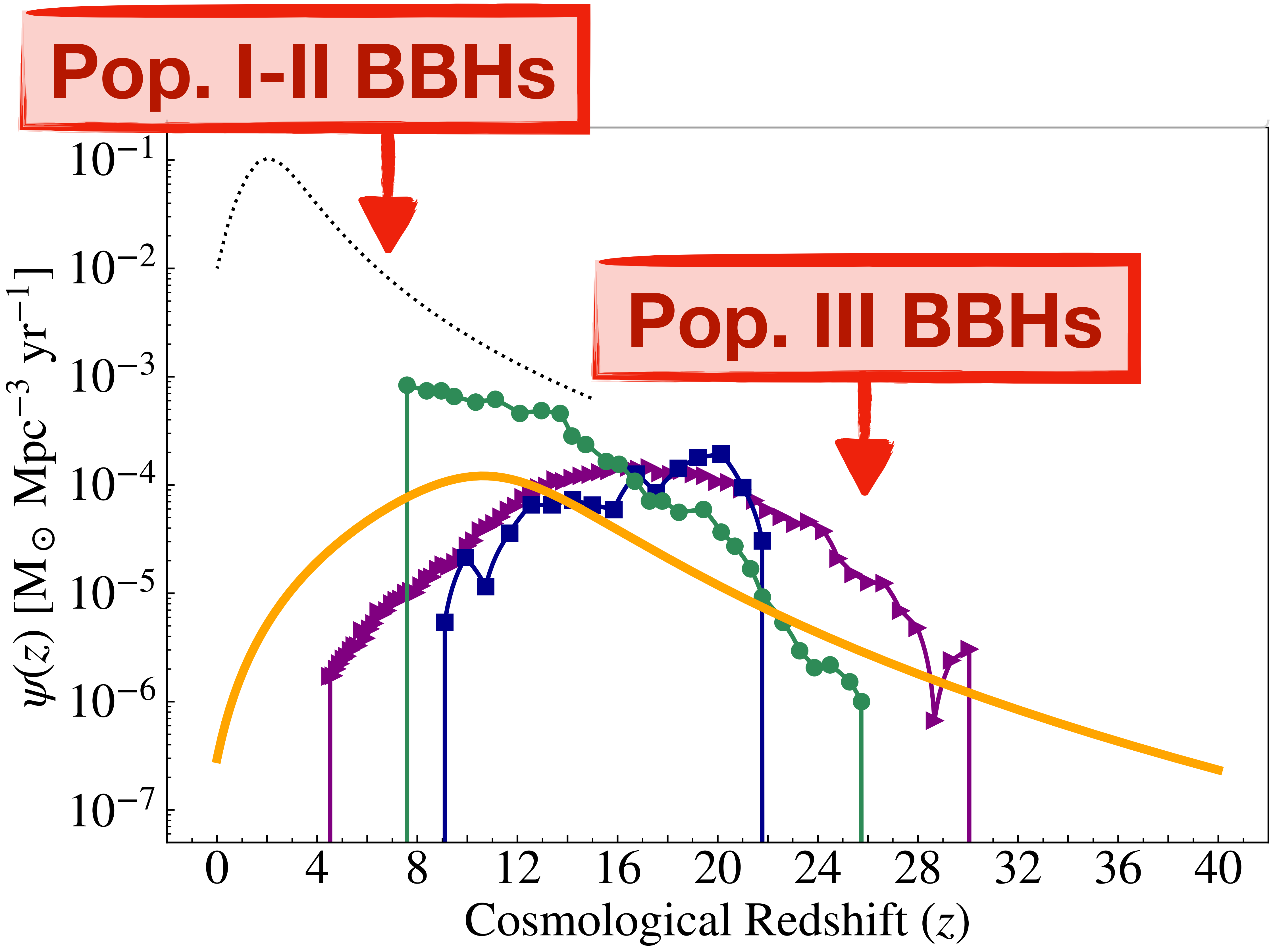

Simulation-based classification

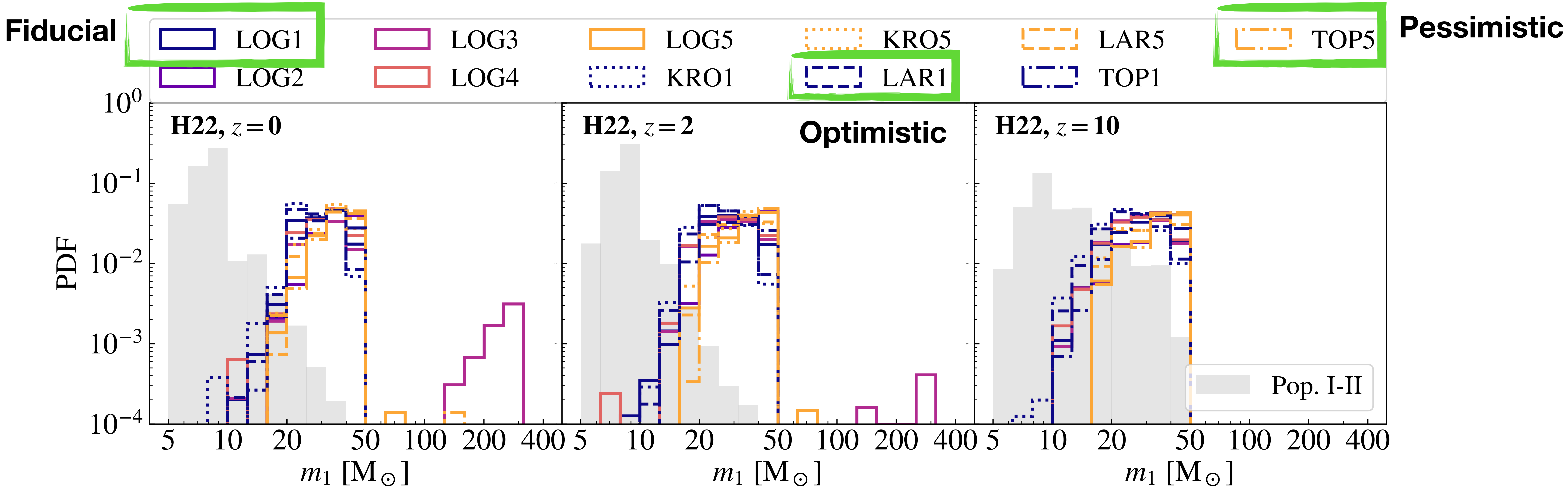

Filippo Santoliquido

Classification

This is the probability that the event j is a Pop. III BBH

$$p(j \in k \,|\, d_i, \{\beta\}) = \int p(j \in k \,|\, x, d_j, \{\beta\})\; p(x \,|\, d_j, \{\beta\})$$

Mixing fraction

Fiducial ~4% $\beta_{III} \propto N_{\text{Pop. III}} \sim 400$

$\beta_{I-II} \propto N_{\text{Pop. I–II}} \sim 10^4$

Classification

$$p(j \in k \mid d_i, \{\beta\}) = \int p(j \in k \mid x, d_j, \{\beta\})\, p(x \mid d_j, \{\beta\})$$

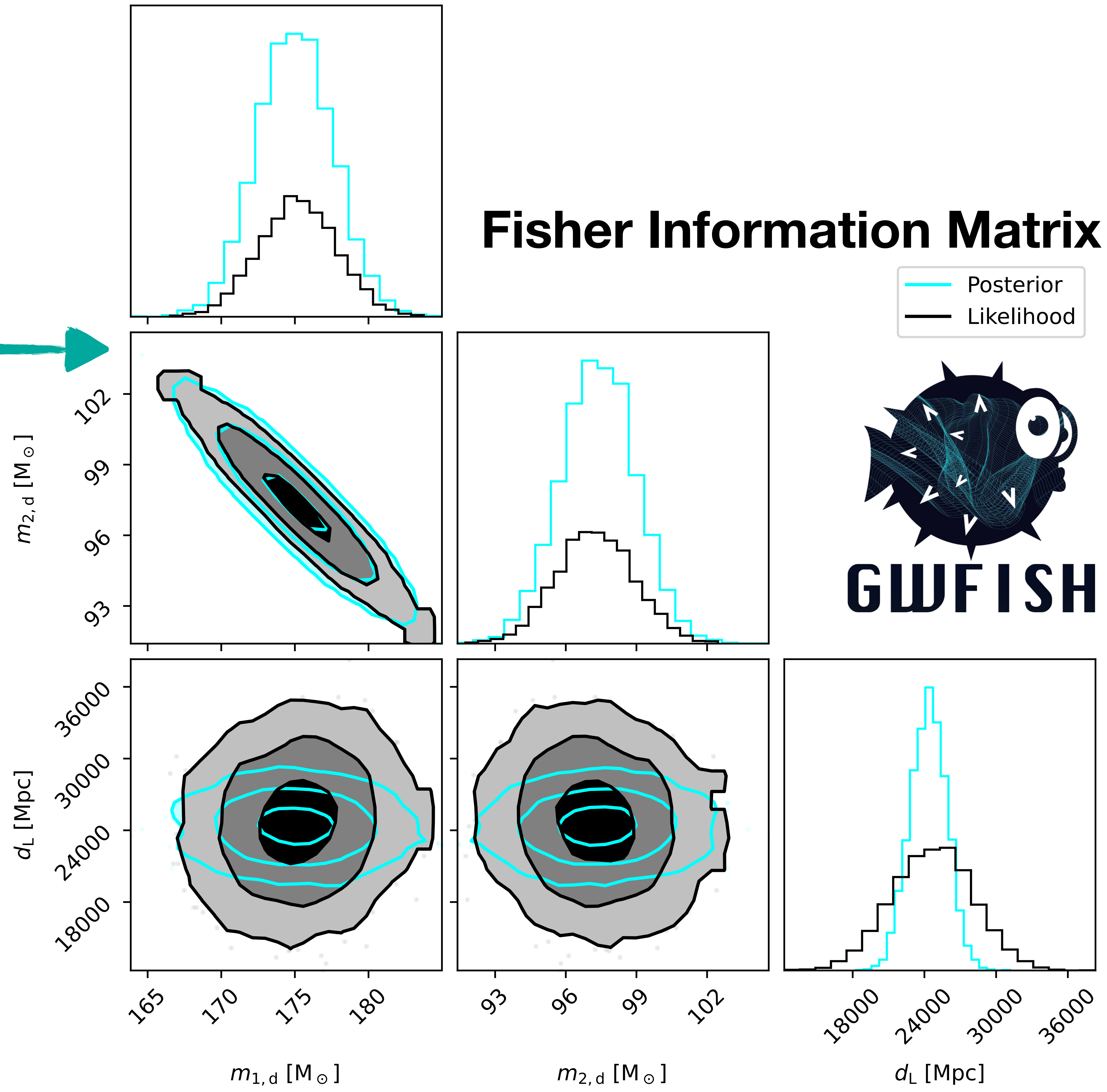

This is the posterior of waveform parameters ➡️ parameter estimation **performance of ET**

Classification

$$p(j \in k \,|\, d_i, \{\beta\}) = \int p(j \in k \,|\, x, d_j, \{\beta\})\, p(x \,|\, d_j, \{\beta\})$$

This is the probability that links waveform parameters to Pop. III BBHs

➡️ easy to consider a fix threshold

$$p(j \in k \,|\, d_i, \{\beta\}) = \int p(j \in k \,|\, x, d_j, \{\beta\}) \, p(x \,|\, d_j, \{\beta\})$$

$$= 1 \quad \text{if} \quad m_{1,\mathrm{d}} \gtrsim 60 \ \mathrm{M}_\odot$$

$$m_{1,d} = m_1(1 + z)$$

$$p(j \in k \,|\, d_i, \{\beta\}) = \int p(j \in k \,|\, x, d_j, \{\beta\}) \, p(x \,|\, d_j, \{\beta\})$$

$= 1$ if $m_{1,\mathrm{d}} \gtrsim 60\ \mathrm{M}_\odot$

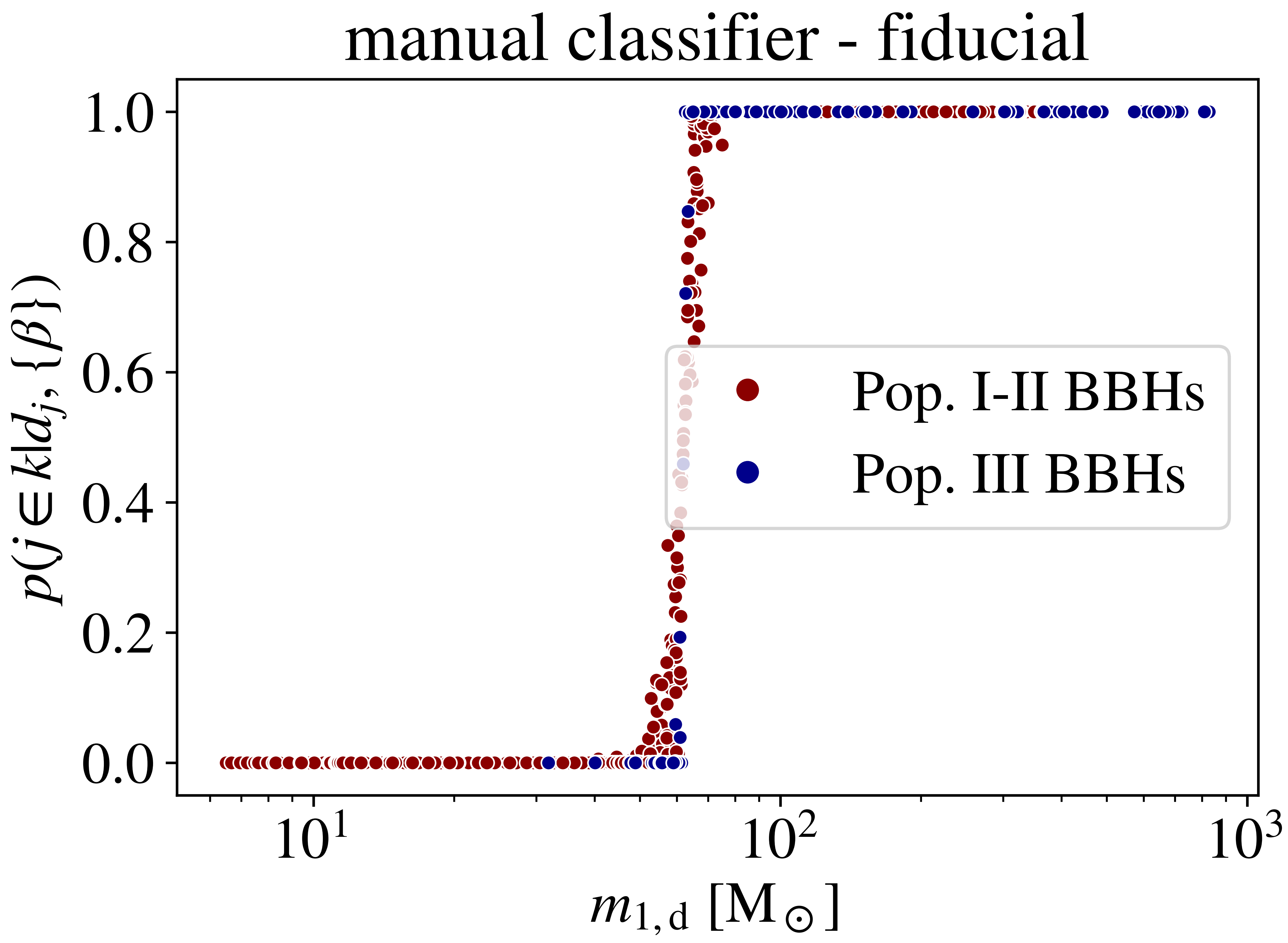

⚠️ low performances: precision is ~ 0.16

$$p(j \in k \,|\, d_i, \{\beta\}) = \int p(j \in k \,|\, x, d_j, \{\beta\}) \, p(x \,|\, d_j, \{\beta\})$$

we can use Machine Learning

XGBoost

supervised ML based on decision trees

Ref. *Santoliquido et al. 2024*, *Chen et al. 2016*, *Pedregosa et al. 2012*, *Antonelli et. al 2023*

$$p(j \in k \,|\, d_i, \{\beta\}) = \int p(j \in k \,|\, x, d_j, \{\beta\}) \, p(x \,|\, d_j, \{\beta\})$$

Using Machine Learning

* trained and tested on balanced classes + re-balancing

* instances: $> 10^4$

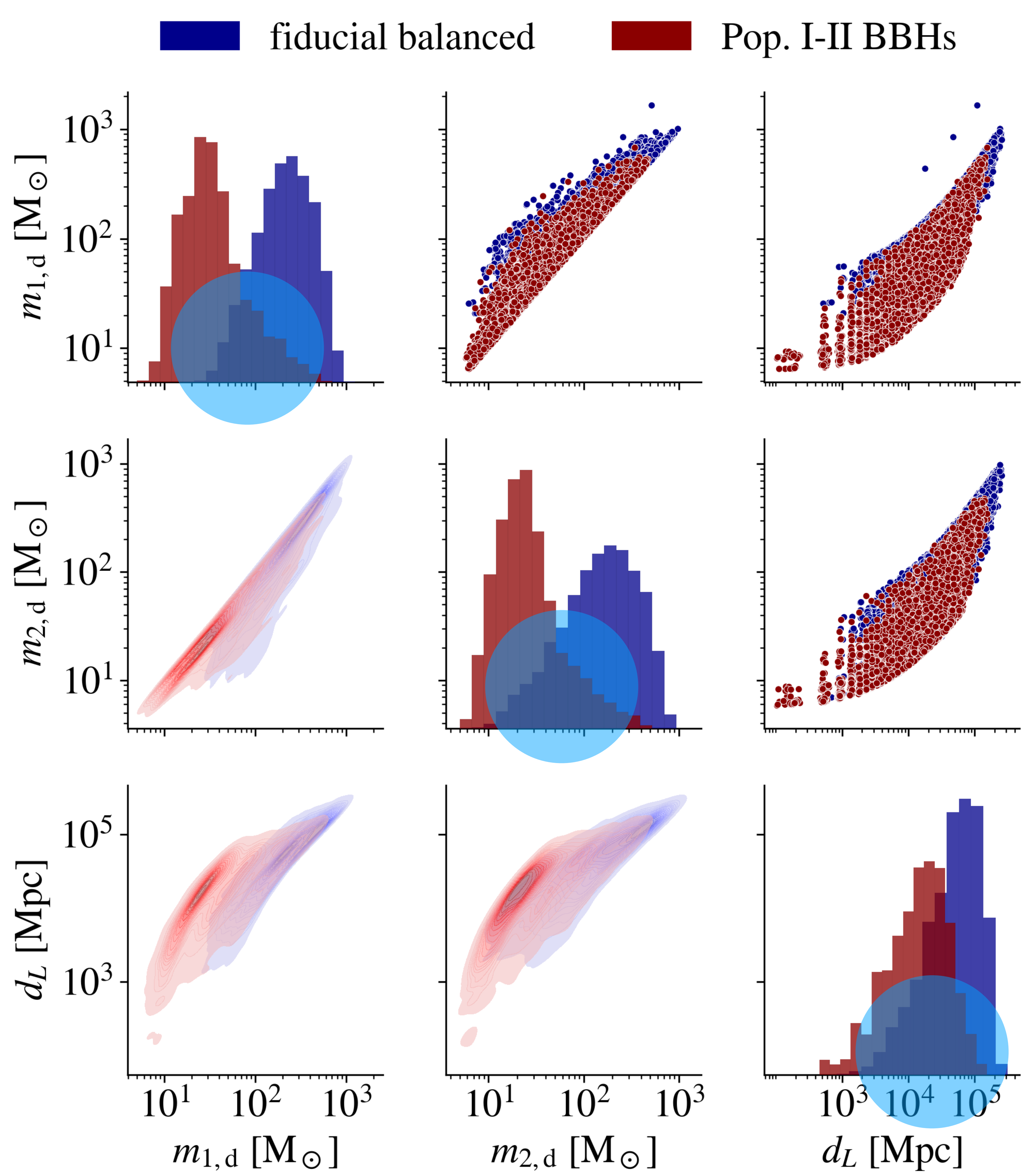

$$p(j \in k \,|\, d_i, \{\beta\}) = \int p(j \in k \,|\, x, d_j, \{\beta\}) \, p(x \,|\, d_j, \{\beta\})$$

Using Machine Learning

precision = TP/(TP+FP)

high precision > 0.90

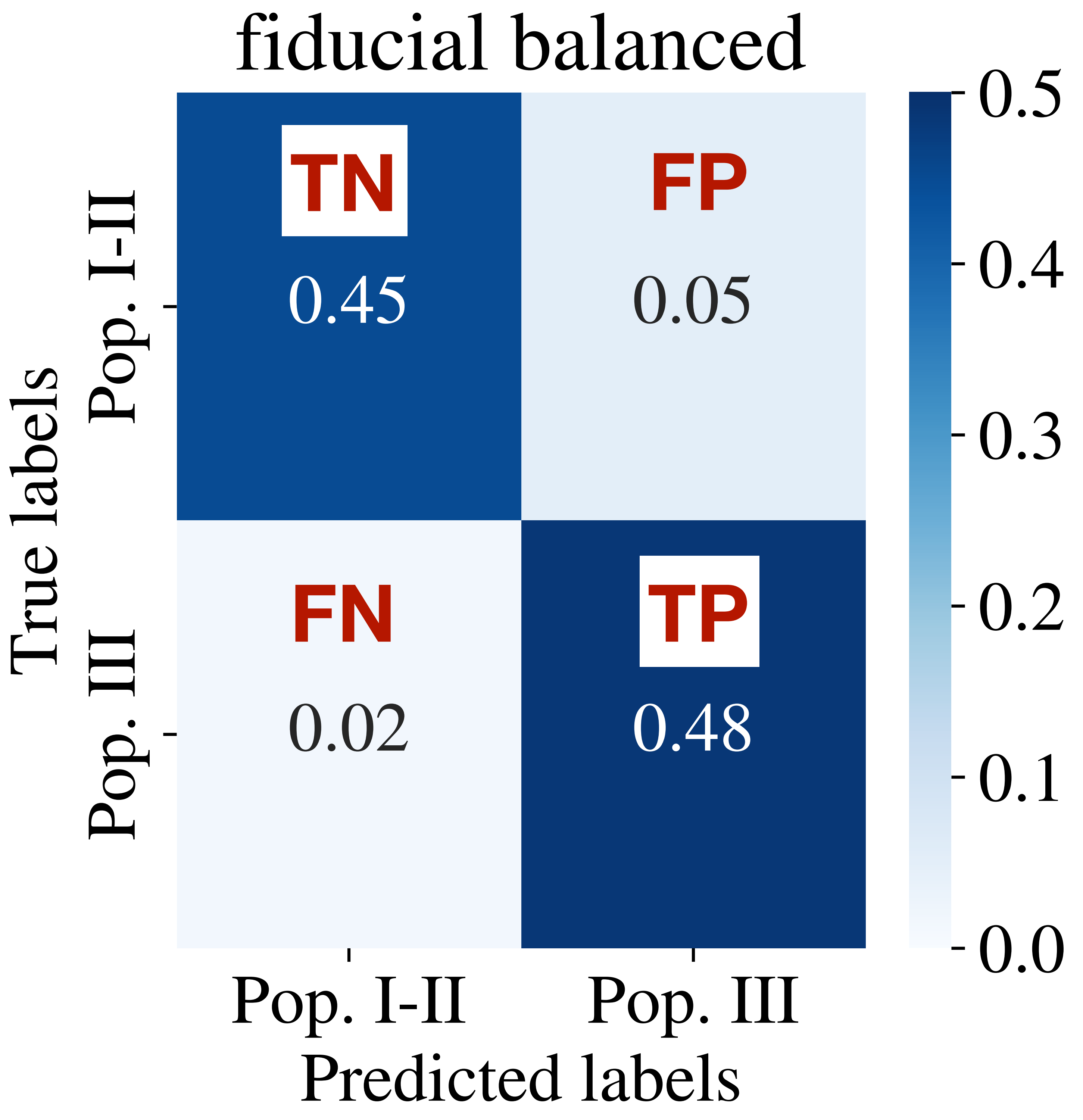

$$p(j \in k \,|\, d_i, \{\beta\}) = \int p(j \in k \,|\, x, d_j, \{\beta\})\, p(x \,|\, d_j, \{\beta\})$$

Using Machine Learning

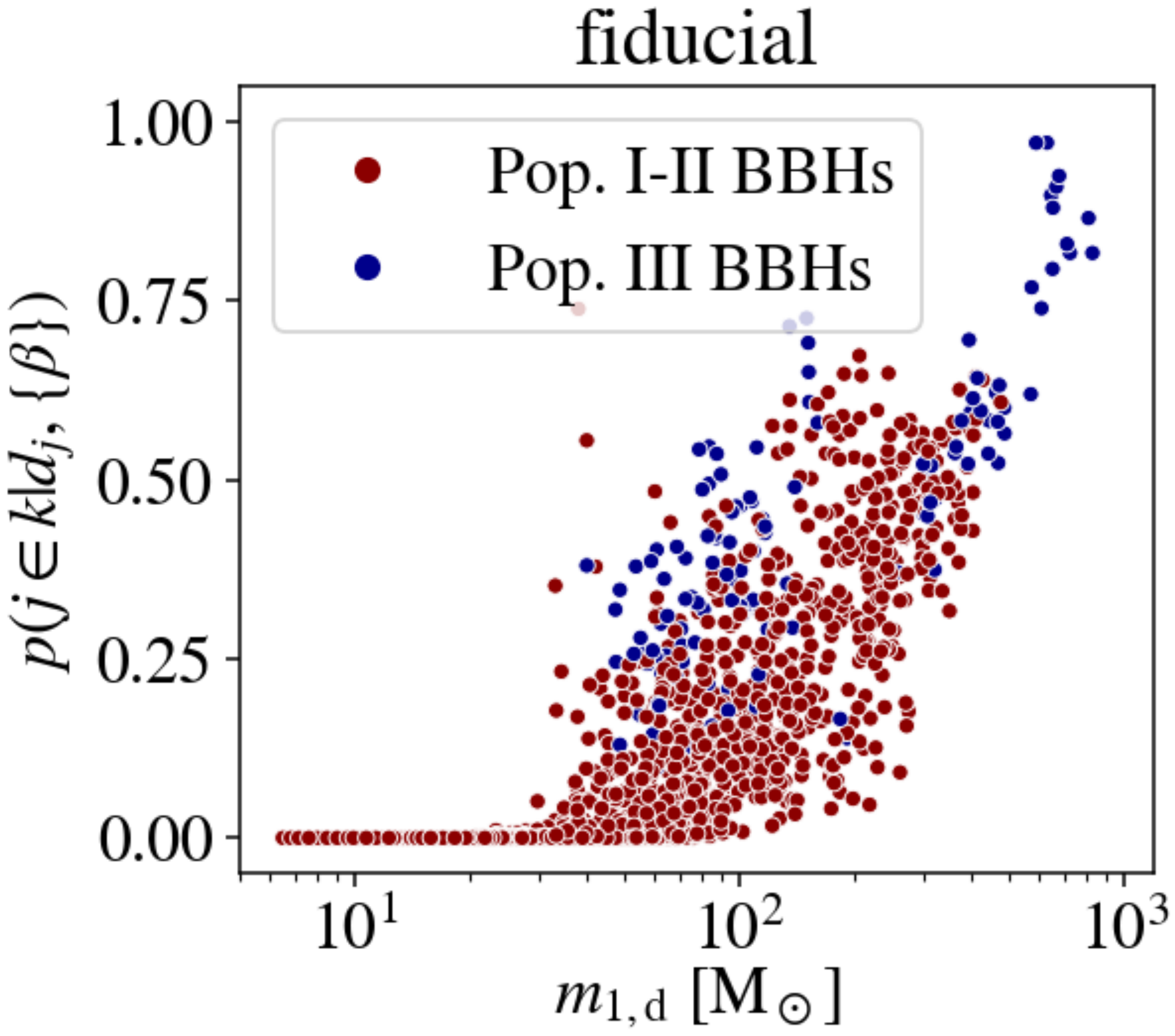

~10% of detected sources are classified with precision > 0.90

$$p(j \in k \,|\, d_i, \{\beta\}) = \int p(j \in k \,|\, x, d_j, \{\beta\})\, p(x \,|\, d_j, \{\beta\})$$

Using Machine Learning

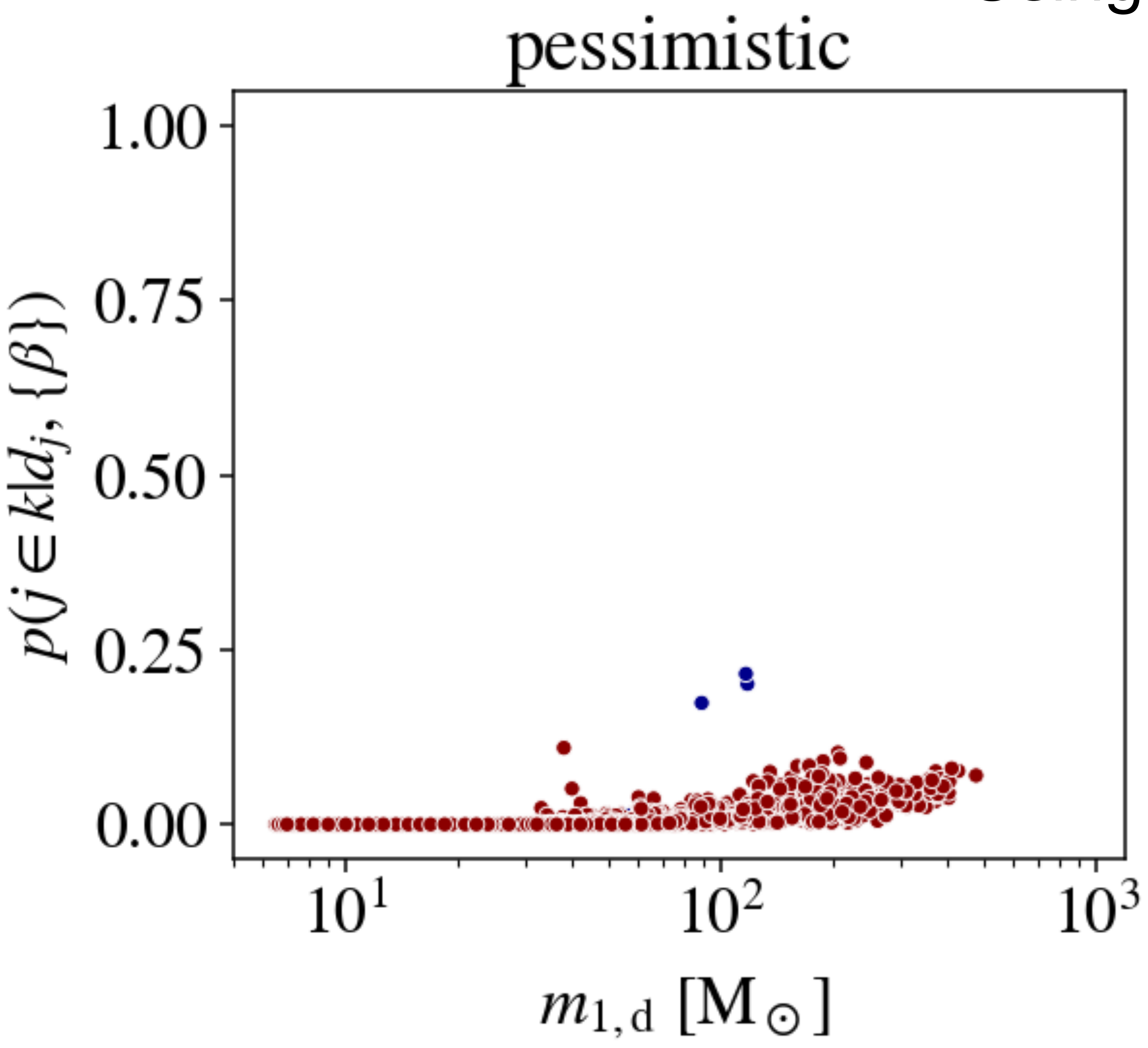

~30% of detected sources are classified with precision > 0.90

$$p(j \in k \mid d_i, \{\beta\}) = \int p(j \in k \mid x, d_j, \{\beta\})\, p(x \mid d_j, \{\beta\})$$

Using Machine Learning

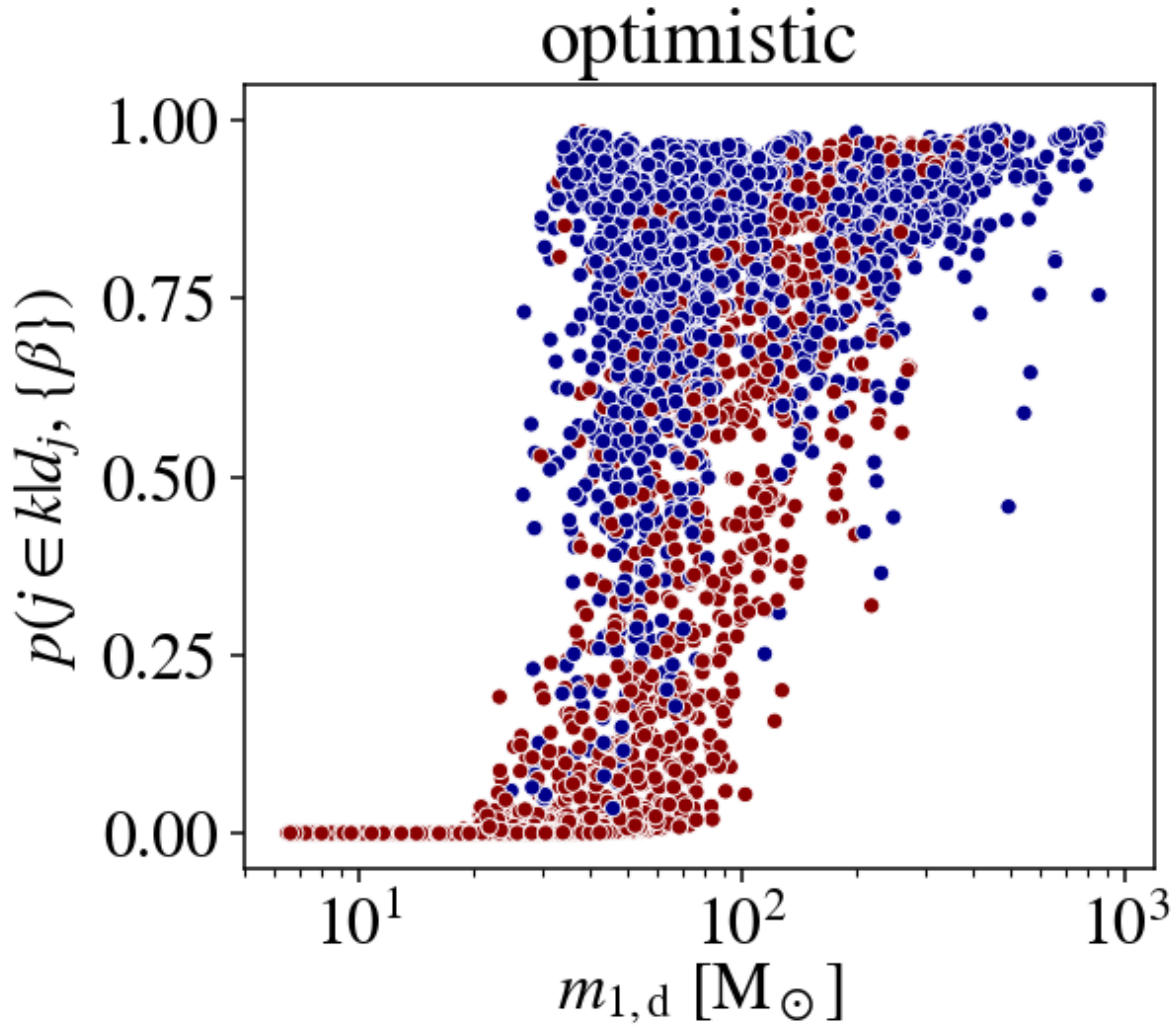

~45% of detected sources are classified with precision > 0.90

Contributions

- First large parameter exploration of Pop. III BBHs
  - SFRD affects normalisation and shape of merger rate density
  - primary mass of Pop. III BHs is substantially massive
- ET will detect these sources and machine learning boosts our ability to classify them

Ref. ***Costa et al. 2023***, ***Santoliquido et al. 2023***, ***Santoliquido et al. 2024***

Backup slides

αλ formalism for modelling the common envelope

- $\Delta E = \alpha(E_{\rm b,f} - E_{\rm b,i}) = \alpha \frac{G m_{\rm c1} m_{\rm c2}}{2} \left(\frac{1}{a_{\rm f}} - \frac{1}{a_{\rm i}} \right)$ This is the orbital energy before and after the common envelope phase
- $E_{\rm env} = \frac{G}{\lambda} \left[\frac{m_{\rm env,1} m_1}{R_1} + \frac{m_{\rm env,2} m_2}{R_2} \right]$ This is the binding energy of the envelope
- By imposing $\Delta E = E_{\rm env}$, $\frac{1}{a_{\rm f}} = \frac{1}{\alpha\lambda} \frac{2}{m_{\rm c1} m_{\rm c2}} \left[\frac{m_{\rm env,1} m_1}{R_1} + \frac{m_{\rm env,2} m_2}{R_2} \right] + \frac{1}{a_i}$
- If α is larger, $a_{\rm f}$ is larger, following $a_{\rm f} \sim \frac{\alpha}{1+\alpha}$. Therefore larger α gets wider binaries
- Where λ is the parameter which measures the concentration of the envelope (the smaller λ is, the more concentrated is the envelope).
- The $\alpha\lambda$ formalism is a simplified prescription. When $\alpha > 1$, we account for other sources of energy that make the envelope less bind, for instance recombination energy. Recent works (e.g. *Fragos et al. 2019*) suggest that $\alpha > 1$ is necessary to reproduce the final orbital separation obtained with hydrodynamical simulations.

Initial conditions

Table 1. Initial conditions.

Model	$M_{ZAMS,1}$	M_{ZAMS}	q	P	e
LOG1	Flat in log	–	S12	S12	S12
LOG2	Flat in log	–	S12	SB13	Thermal
LOG3	–	Flat in log	Sorted	S12	S12
LOG4	Flat in log	–	SB13	S12	Thermal
LOG5	Flat in log	–	SB13	SB13	Thermal
KRO1	K01	–	S12	S12	S12
KRO5	K01	–	SB13	SB13	Thermal
LAR1	L98	–	S12	S12	S12
LAR5	L98	–	SB13	SB13	Thermal
TOP1	Top heavy	–	S12	S12	S12
TOP5	Top heavy	–	SB13	SB13	Thermal

Column 1 reports the model name. Column 2 describes how we generate the ZAMS mass of the primary star (i.e., the most massive of the two members of the binary system). Column 3 describes how we generate the ZAMS mass of the overall stellar population (without differentiating between primary and secondary stars). We follow this procedure only for model LOG3 (see the text for details). Columns 4, 5, and 6 specify the distributions we used to generate the mass ratios q, the orbital periods P and the orbital eccentricity e. See Section 2.2 for a detailed description of these distributions.

Santoliquido et al. 2023:
https://arxiv.org/pdf/2303.15515.pdf

Pop. III BBHs: mass evolution

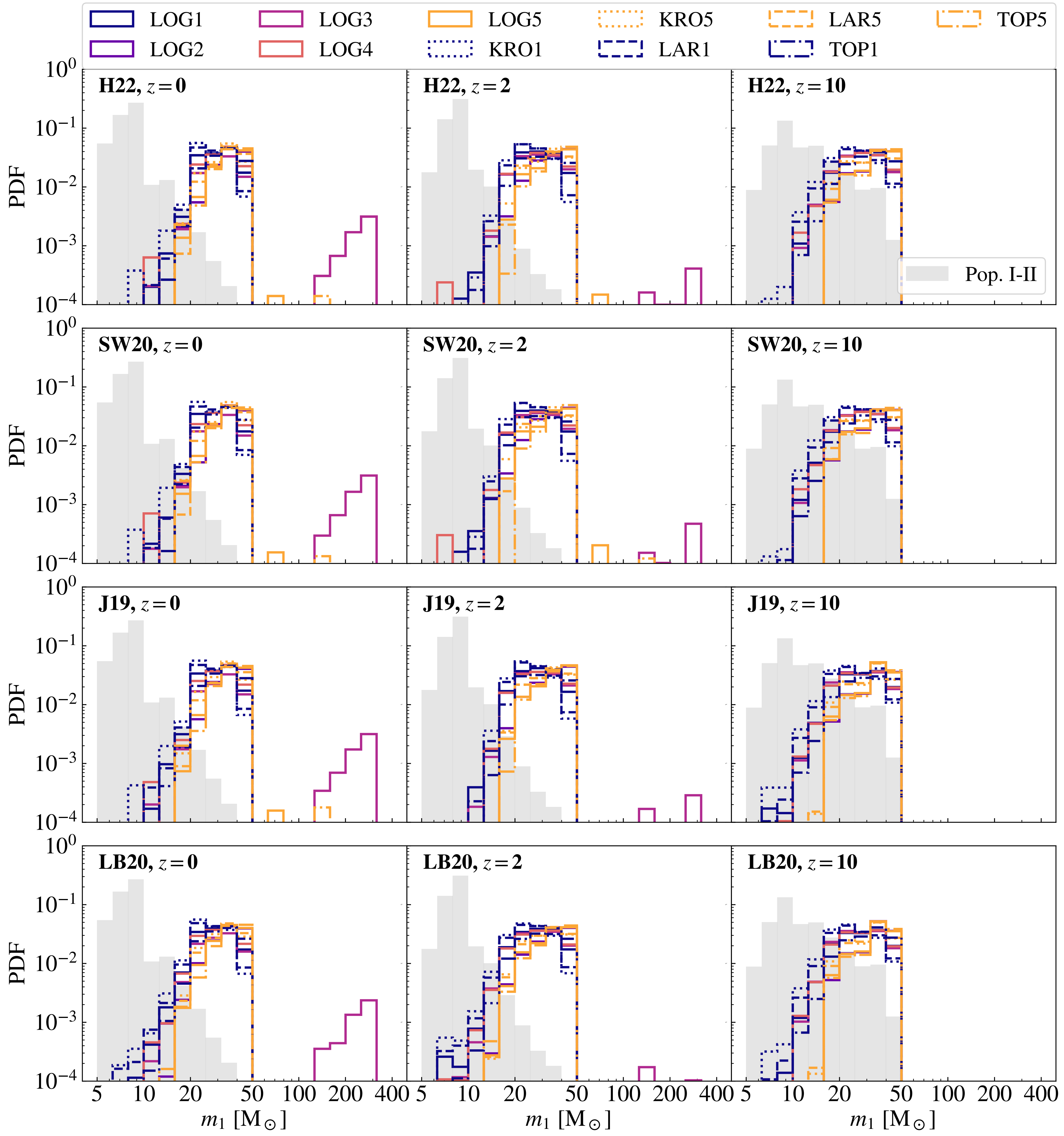

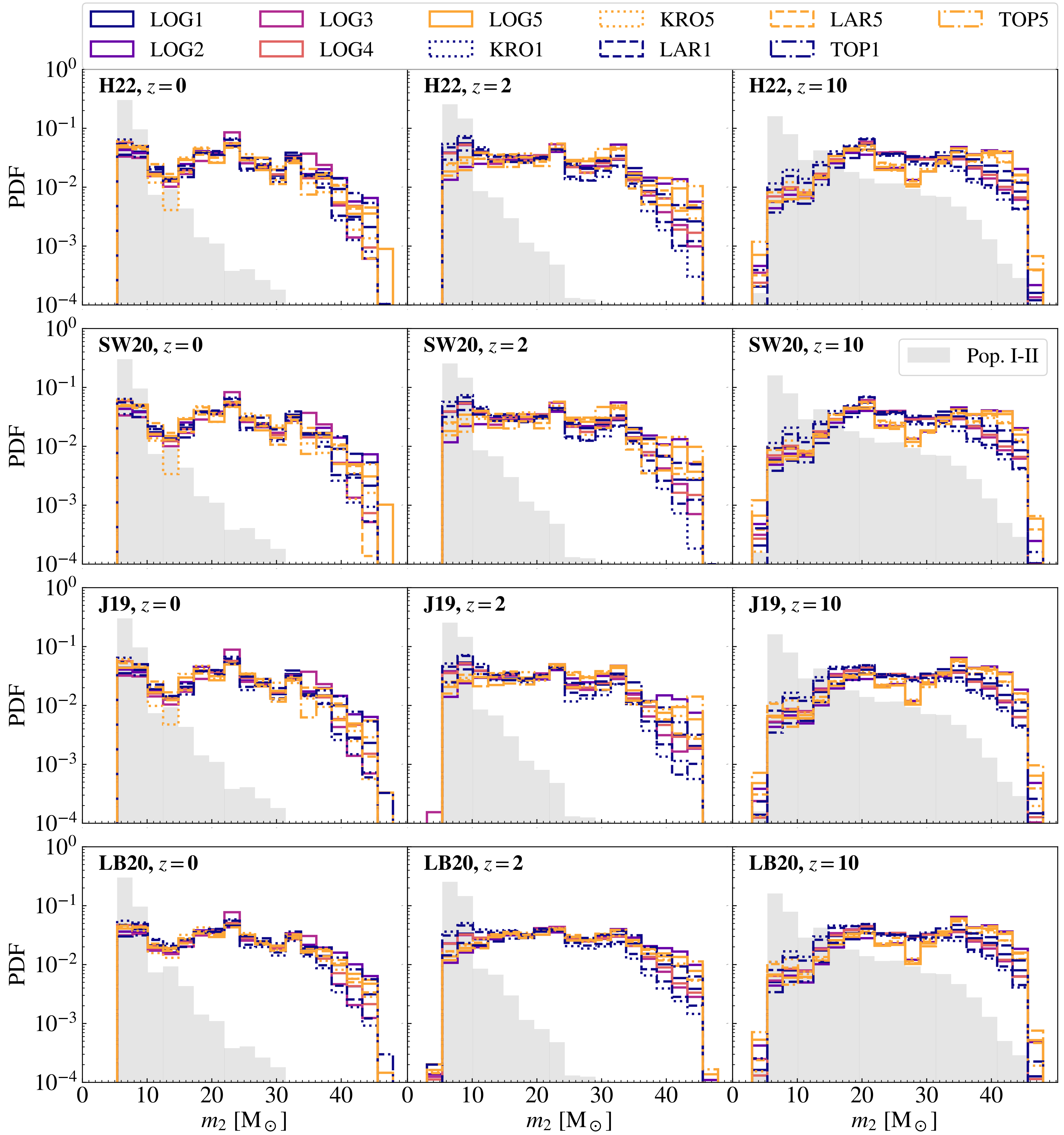

detection rate

$$\mathcal{R}_{\rm det} = \int \frac{{\rm d}^2\mathcal{R}(m_1, m_2, z)}{{\rm d}m_1 {\rm d}m_2} \frac{1}{(1+z)} \frac{{\rm d}V_c}{{\rm d}z}\, p_{\rm det}(m_1, m_2, z)\, {\rm d}m_1\, {\rm d}m_2\, {\rm d}z$$

$$\frac{{\rm d}^2\mathcal{R}(m_1, m_2, z)}{{\rm d}m_1 {\rm d}m_2} = \mathcal{R}(z)\, p(m_1, m_2|z)$$

$$\rho = \rho_{\rm opt} \sqrt{\omega_0^2 + \omega_1^2 + \omega_2^2}$$

$$\rho_{\rm opt}^2 = 4 \int_{f_{\rm low}}^{f_{\rm high}} {\rm d}f\, \frac{|\tilde{h}(f)|^2}{S_n(f)}$$

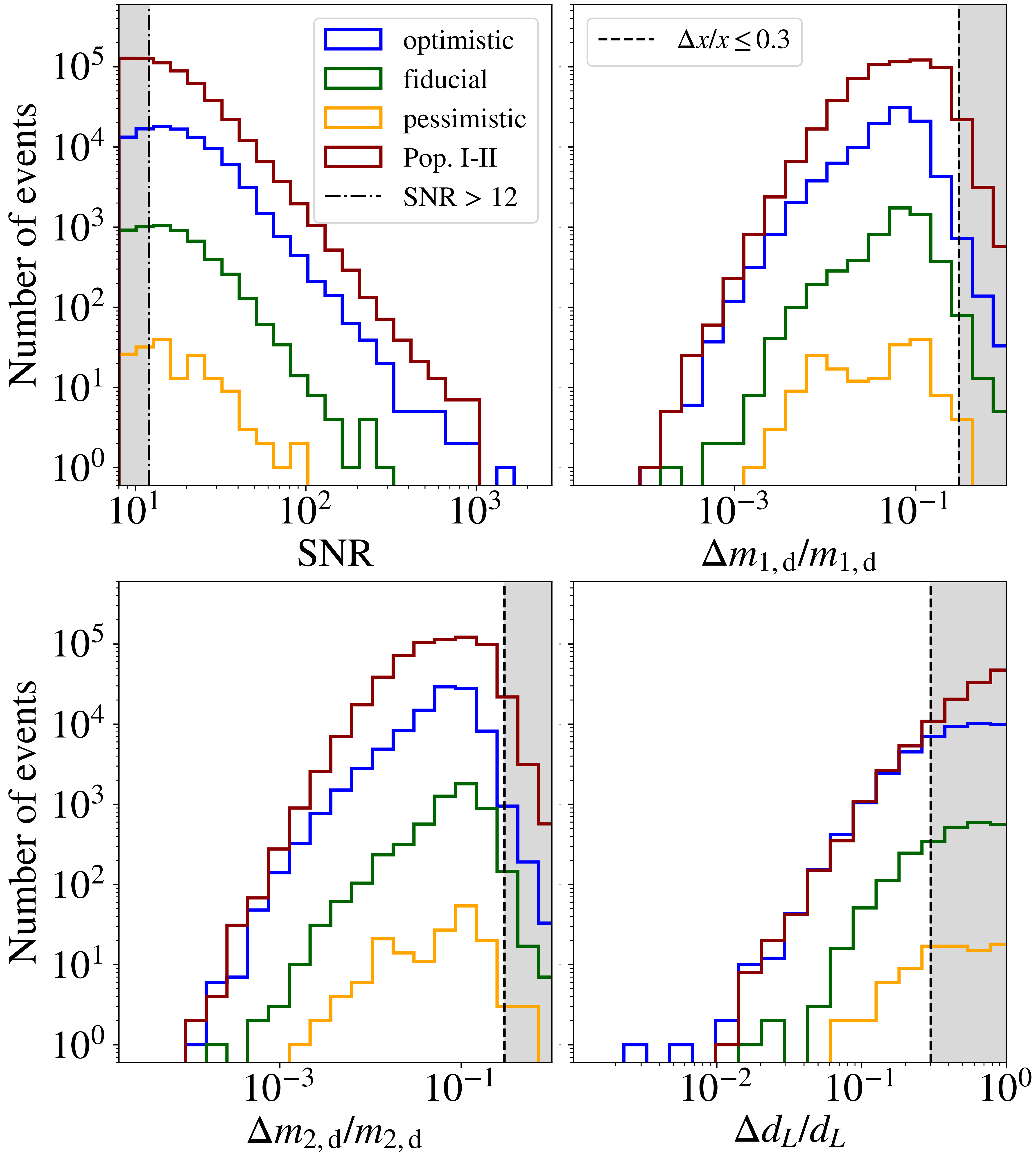

Number of events
SNR
optimistic
fiducial
pessimistic
Pop. I-II
SNR > 12
$\Delta x/x \leq 0.3$
$\Delta m_{1,\mathrm{d}}/m_{1,\mathrm{d}}$
Number of events
$\Delta m_{2,\mathrm{d}}/m_{2,\mathrm{d}}$
$\Delta d_L/d_L$

$$p(j \in k \,|\, x, d_j, \{\beta\}) = 1 \quad \text{if} \quad m_{1,\mathrm{d}} \gtrsim 60\ \mathrm{M}_\odot$$

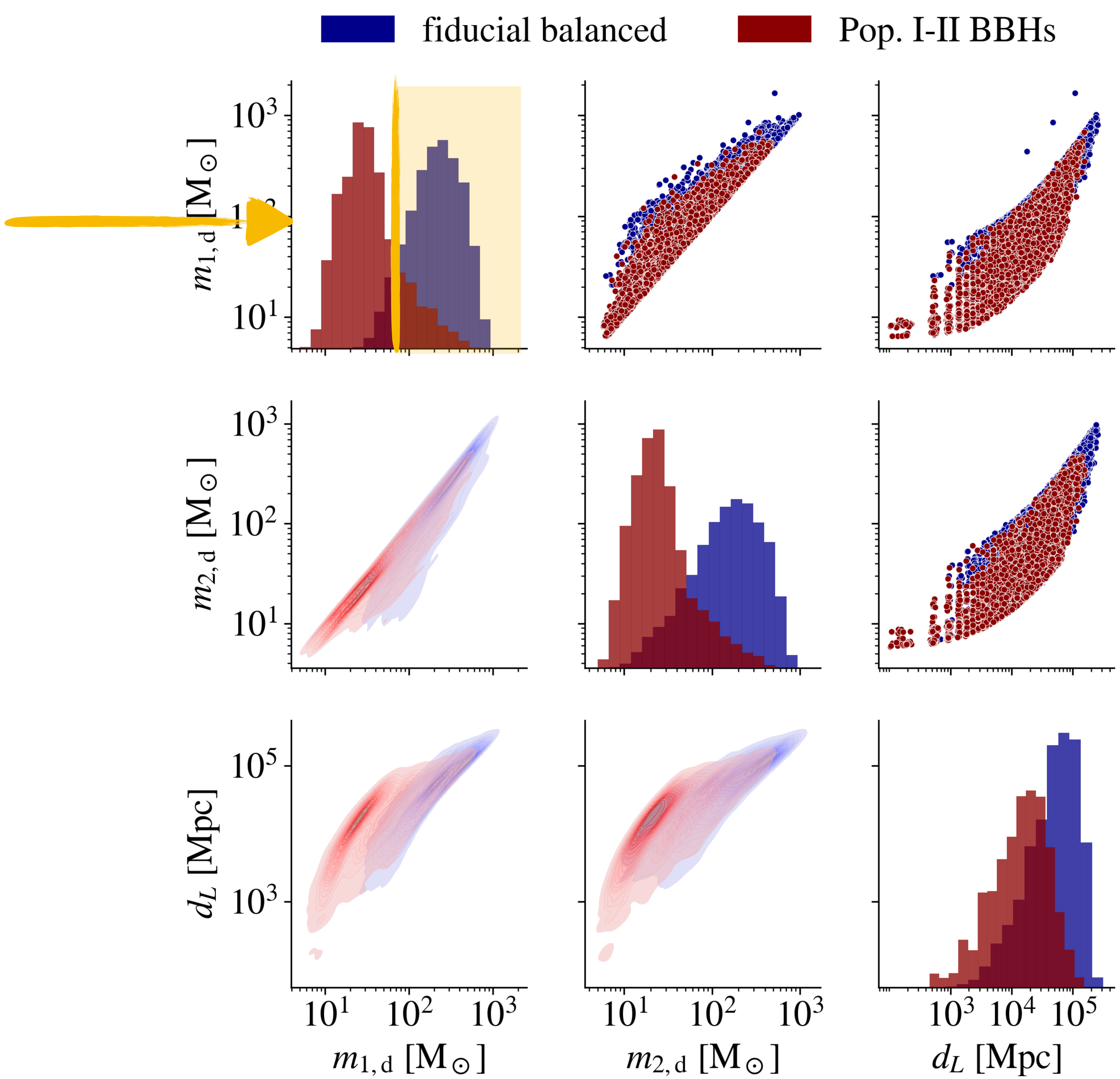

Ref. ***Santoliquido et al. 2024***

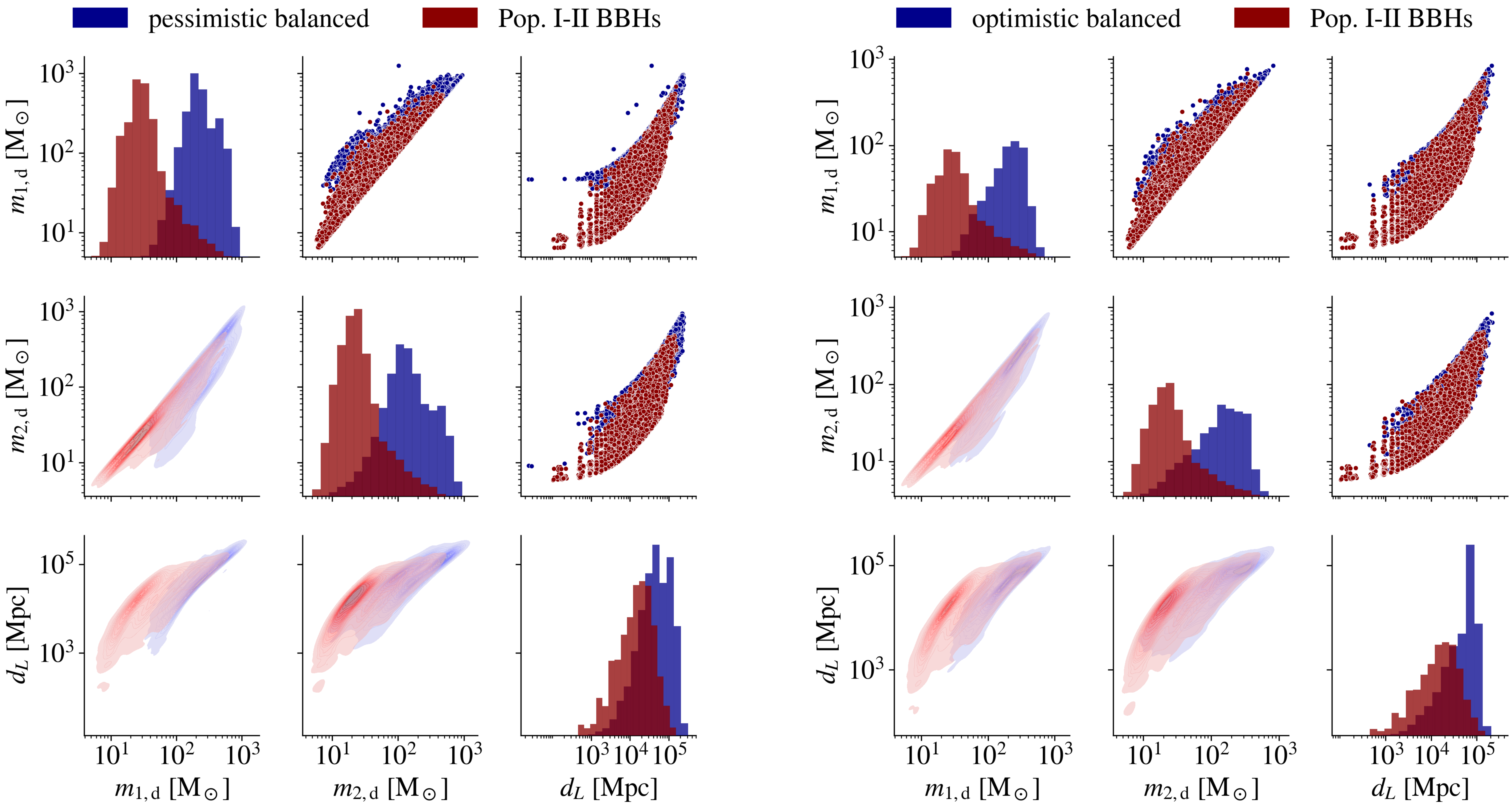
pessimistic balanced
Pop. I-II BBHs
optimistic balanced
Pop. I-II BBHs
$m_{1,\mathrm{d}}$ [M$_\odot$]
$m_{2,\mathrm{d}}$ [M$_\odot$]
d_L [Mpc]
10^1
10^2
10^3
10^4
10^5

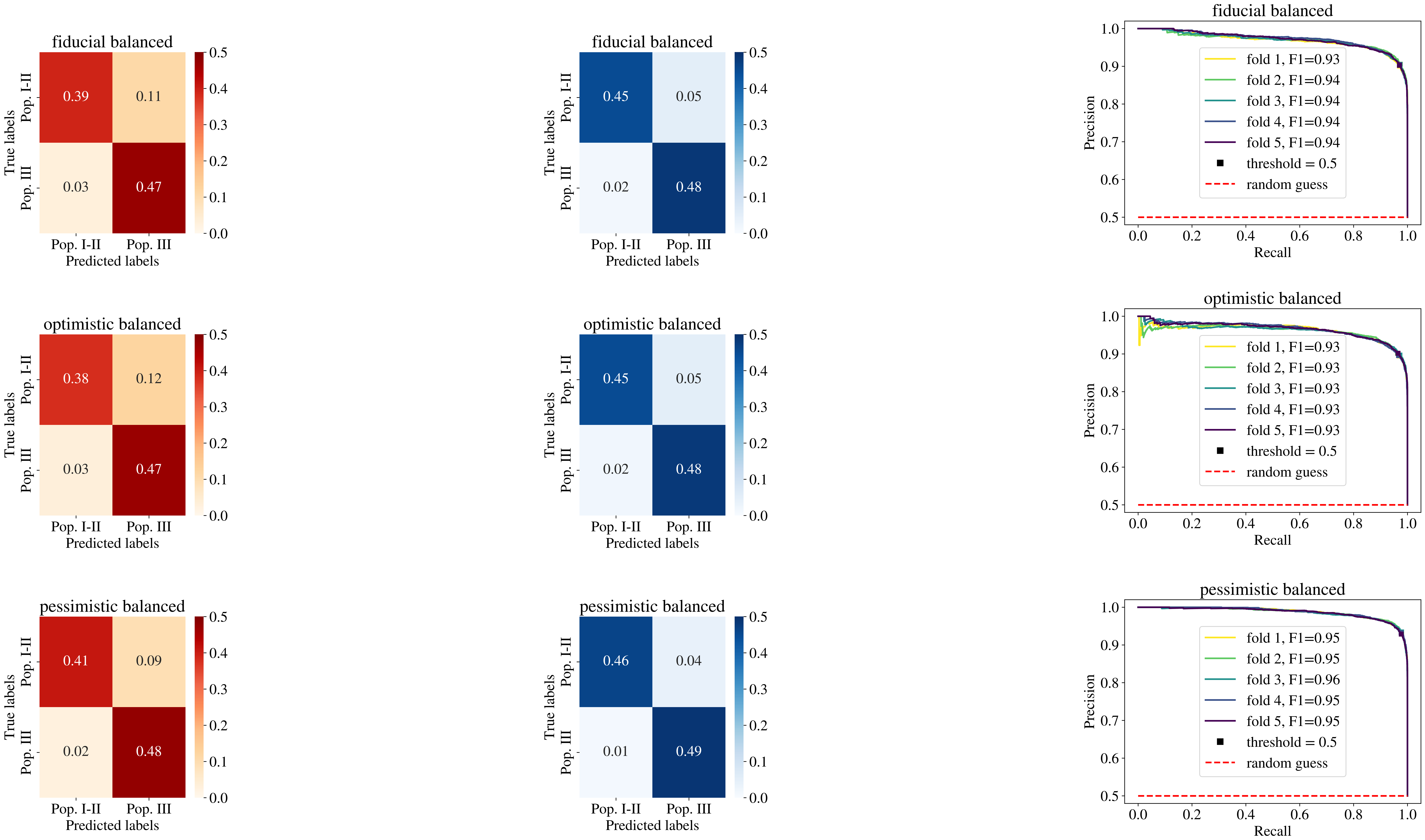
fiducial balanced
True labels
Predicted labels
Pop. I-II
Pop. III
0.39
0.11
0.03
0.47
0.0
0.1
0.2
0.3
0.4
0.5
fiducial balanced
0.45
0.05
0.02
0.48
fiducial balanced
Precision
Recall
fold 1, F1=0.93
fold 2, F1=0.94
fold 3, F1=0.94
fold 4, F1=0.94
fold 5, F1=0.94
threshold = 0.5
random guess
optimistic balanced
0.38
0.12
0.03
0.47
optimistic balanced
0.45
0.05
0.02
0.48
optimistic balanced
fold 1, F1=0.93
fold 2, F1=0.93
fold 3, F1=0.93
fold 4, F1=0.93
fold 5, F1=0.93
threshold = 0.5
random guess
pessimistic balanced
0.41
0.09
0.02
0.48
pessimistic balanced
0.46
0.04
0.01
0.49
pessimistic balanced
fold 1, F1=0.95
fold 2, F1=0.95
fold 3, F1=0.96
fold 4, F1=0.95
fold 5, F1=0.95
threshold = 0.5
random guess
0.6
0.7
0.8
0.9
1.0

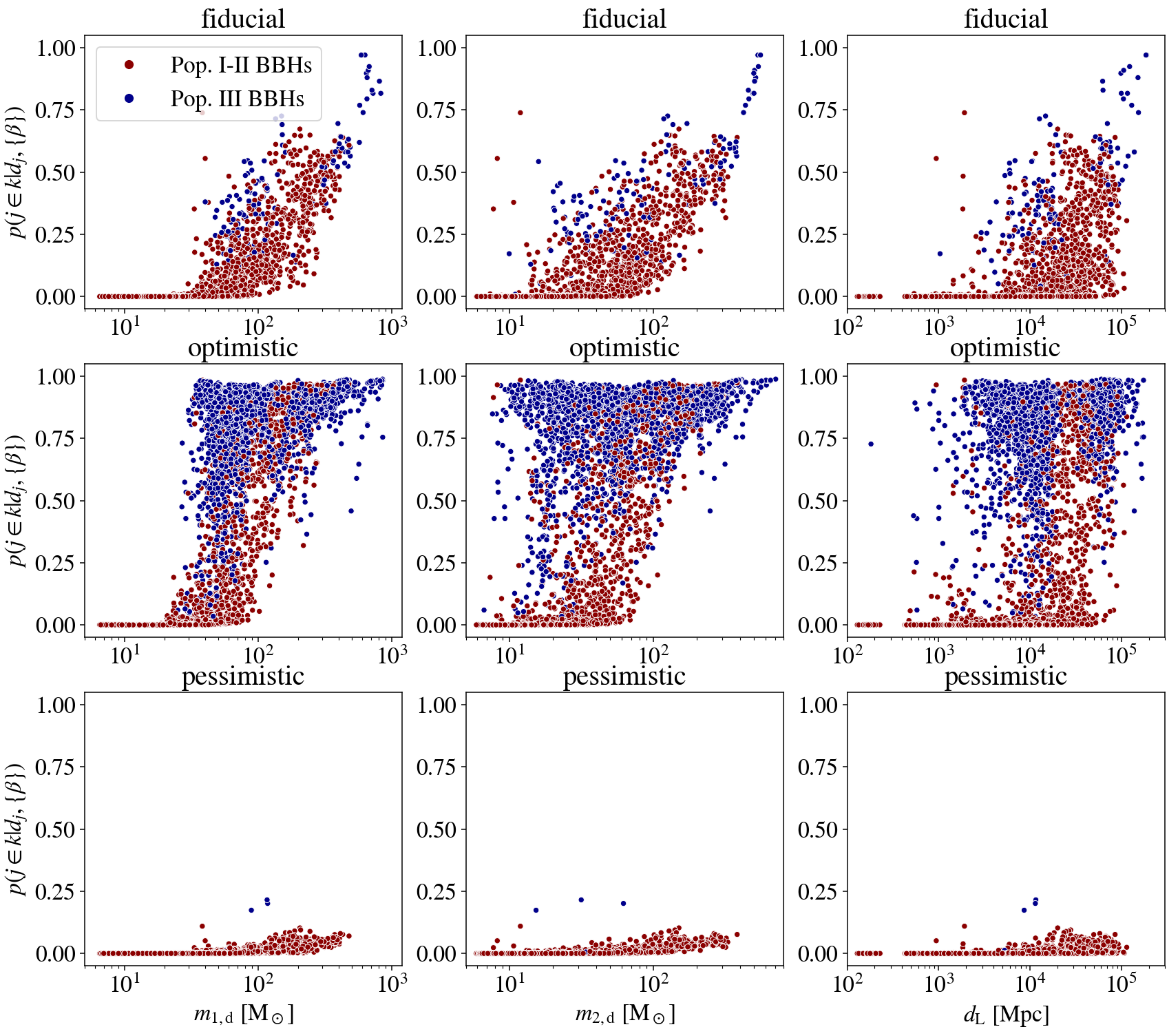

Fiducial

Thr.	%TP	%TN	%FP	%FN	Precision	Recall
0.1	96	85	15	4	0.20	0.96
0.2	86	90	10	14	0.26	0.86
0.5	33	98	2	67	0.43	0.33
0.7	11	100	0	89	0.94	0.11
0.9	3	100	0	97	1.00	0.03

Optimistic

Thr.	%TP	%TN	%FP	%FN	Precision	Recall
0.1	100	77	23	0	0.80	1.00
0.2	99	80	20	1	0.81	0.99
0.5	95	85	15	5	0.85	0.95
0.7	87	89	11	13	0.88	0.87
0.9	46	96	4	54	0.91	0.46

Pessimistic

Thr.	%TP	%TN	%FP	%FN	Precision	Recall
0.1	50	100	0	50	0.60	0.50
0.2	33	100	0	67	1.00	0.33
0.5	0	100	0	100	0	0
0.7	0	100	0	100	0	0
0.9	0	100	0	100	0	0